FUNCTIONAL ANALYSIS OF PRAF1 AND ITS EFFECT ON CORTICOTROPHIC ACTH SECRETION

Except where reference is made to the work of others, the work described in this dissertation is my own or was done in collaboration with my advisory committee. This dissertation does not include proprietary or classified information.

_____

Shannon Leigh Compton

Certificate of Approval:

_____	_____
Robert J. Kemppainen Professor Anatomy, Physiology, & Pharmacology	Ellen N. Behrend, Chair Associate Professor Clinical Sciences
_____	_____
Marie W. Wooten Professor Biological Sciences	Edward E. Morrison Professor Anatomy, Physiology, & Pharmacology

_____

Joe F. Pittman
Interim Dean
Graduate School

FUNCTIONAL ANALYSIS OF PRAF1 AND ITS EFFECT ON CORTICOTROPHIC ACTH SECRETION

Shannon Leigh Compton

A Dissertation

Submitted to

the Graduate Faculty of

Auburn University

in Partial Fulfillment of the

Requirements for the

Degree of

Doctor of Philosophy

Auburn, Alabama
August 4, 2007

FUNCTIONAL ANALYSIS OF PRAF1 AND ITS EFFECT ON CORTICOTROPHIC

ACTH SECRETION

Shannon Leigh Compton

_____
Signature of Author

_____
Date of Graduation

DISSERTATION ABSTRACT

FUNCTIONAL ANALYSIS OF PRAF1 AND ITS EFFECT ON CORTICOTROPHIC ACTH SECRETION

Shannon Leigh Compton

Doctor of Philosophy, August 4, 2007
(M.S. Auburn University, 1999)
(M.Z.S. Auburn University, 1999)
(B.S. Auburn University, 1981)

111 Typed Pages

Directed by Ellen N. Behrend

Prenylated Rab acceptor domain family member 1 (PRAF1), a transmembrane Golgi apparatus protein, interacts with Dexras1, a corticotrophic protein that may play a role in glucocorticoid-mediated inhibition of ACTH secretion. The purpose of this study was to evaluate the effect of mutating PRAF1 on Dexras1 interaction, PRAF1 and ACTH localization, cell morphology, ACTH secretion, and processing and transcription of POMC, the precursor of ACTH.

PCR and site-directed mutagenesis were used to generate the PRAF1 mutations PRAF(54-175), PRAF(54-112), PRAF(N70T), PRAF(Y73A), and PRAF(V161A). Yeast two-hybrid assay was used to assess Dexras1/PRAF1 mutant interaction. PRAF1(54-112) did not interact with Dexras1, however PRAF(54-175) did.[1] The Dexras1

interaction was enhanced in the 3 point mutated proteins, PRAF(N70T), PRAF(Y73A), and PRAF(V161A).

AtT-20 cells were stably transfected with either empty vector (3X) or an expression vector containing mutated or full-length (FL) PRAF1. Basal secretion, CRH-stimulated secretion and the effect of dexamethasone (Dex) on stimulated secretion were studied in wild type (WT) and transfected cells. In WT, and cells stably transfected with 3X- or FL-containing vectors, CRH increased ACTH secretion compared to basal, and Dex inhibited this response. The response to CRH and Dex was significantly altered in all cell lines stably transfected with a PRAF1 mutant construct.

Confocal microscopy revealed that PRAF1 and ACTH localization was altered in all cell lines stably transfected with a PRAF1 mutant construct. Further, the Golgi complex morphology was altered in 2 cell lines. Stable transfection of AtT-20 cells with FL or a PRAF1 mutant increased POMC expression, which was not reflected by an increase in ACTH-containing peptide. However, the ratio of ACTH/pre-ACTH and ACTH/POMC was decreased in all cells stably transfected with a PRAF1 construct except for PRAF(Y73A).

Our results demonstrate that PRAF1 mutations affect PRAF1/Dexras1 interaction, PRAF1 and ACTH localization, Golgi complex morphology, ACTH secretion, and POMC expression and processing. In addition, a PRAF1/Rab3A/VAMP2 interaction may be vital for stimulated secretion of ACTH. Thus, the PRAF1/Dexras1 interaction may play a role in glucocorticoid-mediated inhibition of ACTH secretion in the intermediate time frame.

ACKNOWLEDGEMENTS

I would like to thank my mentor, Dr. Ellen Behrend, and my committee members, Dr. Marie Wooten, Dr. Robert Kemppainen, and Dr. Edward Morrison for their advice and guidance. I would also like to thank Dr. Robert Judd and the members of the Judd lab for the use of their equipment and instruction in the Odyssey system.

I especially want to thank my partner, Michele Smith, not only for her love and support, but also for believing in me.

Style manual or journal used *Nature*

Computer software used Microsoft Office Word (11.6359.6408) SP1

TABLE OF CONTENTS

LIST OF TABLES

LIST OF FIGURES

I. INTRODUCTION

The hypothalamic-pituitary-adrenocortical (HPA) axis is of central importance in normal physiology and is also readily activated by a variety of stresses. Glucocorticoids modulate cellular activity in almost all tissues and play particularly important roles in energy mobilization, maintenance of vascular reactivity, water distribution, and other metabolic functions including resistance or tolerance to stress. As a result, the level of activity of the HPA axis is tightly regulated yet rapidly responsive to changing needs.

Normally, the HPA axis regulates systemic cortisol levels. Briefly, corticotrophin-releasing hormone (CRH) is secreted from the hypothalamus and stimulates ACTH release from the anterior pituitary.[2,3] The adrenal glands respond to adrenocorticotropic hormone (ACTH) by releasing cortisol, which then feeds back to the hypothalamus and anterior pituitary to inhibit CRH secretion and ACTH release, respectively.[4,5] *In vivo*, the effect of glucocorticoids on HPA axis activity can be divided into early, intermediate, and slow domains,[6] while *in vitro* studies of pituitary cells have shown that glucocorticoid negative feedback generally operates in one of two time domains: early and delayed.[6] The early feedback occurs within 0.5-3 hours of cellular exposure to glucocorticoids and continues until the delayed feedback begins, approximately 9 hours after steroid exposure.[7,8] Early *in vitro* effects are the same as *in vivo* intermediate feedback, and will be hereafter referred to as intermediate feedback.

Dysregulation of the HPA axis with increased and/or prolonged activation has been implicated in a number of pathologies, including susceptibility to immune-mediated arthritis in certain strains of rats (potentially related to deficient HPA axis activation secondary to excessive negative feedback) and in humans, melancholic depression, anorexia nervosa, obsessive-compulsive disorder, and panic anxiety.[9] Cushing's disease, one of the best characterized HPA axis diseases, was first described by Henry Cushing in 1932 as hypercortisolism resulting from basophilic adenomas of the pituitary.[10] Currently, Cushing's disease accounts for approximately 70 – 80% of human patients with endogenous hypercortisolism.[11] Most cases are caused by a single ACTH-producing pituitary adenoma, but others are caused by pituitary corticotroph hyperplasia, multiple adenomas, or both.[12-14] Symptoms include protein loss, adiposity, fatigue and weakness, capillary fragility, and edema.

In an attempt to better understand the physiology of the normal feedback mechanism, Kemppainen and Behrend utilized differential display using AtT-20 cells, a murine corticotroph cell line, treated with dexamethasone (Dex) to identify glucocorticoid-induced genes. As a result, Dexras1, a member of the Ras superfamily, was isolated.[15] There is some evidence to indicate that Dexras1 may be implicated in corticotroph negative feedback, although the precise mechanism is unknown.[15,16]

Since one of the best ways to determine a protein's function is to identify the proteins with which it interacts, Dexras1 interactors were sought. A yeast two-hybrid screen identified prenylated Rab accepter domain family member 1 (PRAF1) as a potential Dexras1 interactor.[17] Further, amino acids 54-175 of PRA1 are necessary for interaction with Dexas1, as is the prenylation of Dexras1.[1] Other research identified

Rab3A and VAMP2 as also interacting with PRAF1.[18] A Rab3A/VAMP2 interaction activates VAMP2 and activated VAMP2 is necessary for exocytosis.[18] Thus, a Dexras1/PRAF1 interaction could inhibit glucocorticoid-mediated inhibition of ACTH secretion by affecting the interaction between PRAF1, Rab3A, and VAMP2.

Consequently, the interaction between Dexras1 and PRAF1 is of great interest for furthering our understanding of how normal feedback inhibition works, as well as the implications of abnormalities for illnesses such as Cushing's disease. Accordingly, this interaction was chosen for further research. There were four main objectives guiding this study:

1. Determine the effect of full-length and 2 truncated forms of PRAF1 on PRAF1 localization and ACTH localization and secretion in AtT-20 cells.
2. Characterize the effect of PRAF1 point mutations on PRAF1 localization and ACTH localization and secretion in AtT-20 cells.
3. Determine the effect of PRAF1 point mutations on interaction with Dexras1.
4. Determine the effect, if any, of PRAF1 mutations on POMC transcription or processing.

To achieve these objectives, immunohistochemistry, confocal microscopy, Western blotting, IRMA, and yeast two-hybrid studies were utilized.

The results, reported in Chapter 4 of this dissertation, indicate that mutations in PRAF1 affect PRAF1 and ACTH localization, ACTH secretion, POMC transcription, and POMC processing. Some of the mutations were based on those tested by Gougeon et al.,[19]while others were based on previous results.[1] The mutations were 2 truncated versions: PRAF(54-175) and PRAF(54-112), and three induced point mutations:

PRAF(N70T), PRAF(Y73A), and PRAF(V161A). Of the mutations, only PRAF(54-112) did not interact with Dexras1 in the yeast two-hybrid assay, while amino acids 54-175 of PRAf1 are sufficient for interaction.[1] All 3 point mutations enhanced Dexras1/PRAF1 interaction.

The ACTH IRMA and Western Blots had similar results with regard to the cellular response to CRH and Dexamethasone (Dex). In wild type (WT) AtT-20s and those containing empty vector (3X) or full length (FL) PRAF1, CRH increased ACTH secretion compared to basal concentrations, and Dex inhibited the CRH response. However, in PRAF(54-175), PRAF(54-112), PRAF(N70T), neither CRH nor Dex affected ACTH secretion. Cells transfected with PRAF(Y73A) responded to CRH, but this response was not inhibited by Dex pretreatment. In contrast, cells transfected with mutant PRAF(V161A) had a slight but significant increase in ACTH secretion compared to vehicle treatment, but the opposite response to Dex as that of WT. PRAF1 mutations also altered the overall amount of ACTH that was secreted into the media such that WT, 3X, FL, and PRAF(V161A) were within the same range, whereas PRAF(54-175), PRAF(54-112), PRAF(N70T), and PRAF(Y73A) secreted significantly more. In the cell lysates, the ACTH concentration was significantly higher in WT, 3X, and PRAF(N70T) than in other cell types, and there was no significant difference between treatments within a cell type. The Western blot results also showed that pre-ACTH was secreted into the media of all stable transfectants, whereas pre-ACTH was detected in the lysates of all cell types. In addition, in vehicle treated cells the ratio of ACTH to POMC and pre-ACTH was significantly decreased in FL, PRAF(54-175), PRAF(54-112), and PRAF(Y73A)

compared to WT. However, the ratio of pre-ACTH to POMC was not significantly different in any stable transfectant compared to WT.

The RT-PCR results for 3X stable transfectants revealed that stable transfection does not alter POMC transcription. However, POMC transcription was significantly increased in all other stable transfectants. In FL stable transfectants, POMC transcription was approximately 3 fold higher than in WT and 3X cells, while in PRAF(54-112) and PRAF(Y73A) POMC transcription was approximately 4 fold. Finally, in PRAF(V161A) and PRAF(N70T) POMC transcription was approximately 5 and 6 fold, respectively.

The images obtained via confocal microscopy revealed that PRAF1 localized to the Golgi complex in all cell lines except PRAF(54-112) and PRAF(54-175). In WT, 3X, FL, PRAF(54-175) and PRAF(V161A), the ACTH signal was distributed throughout the cytosol, but was limited to the Golgi complex in PRAF(54-112), PRAF(N70T), and PRAF(Y73A).

These results demonstrate that PRAF1 mutations affect PRAF1/Dexras1 interaction, PRAF1 and ACTH localization, ACTH secretion, POMC transcription, and POMC processing. Thus, it seems likely that PRAF1 does play a role in glucocorticoid-mediated inhibition of ACTH secretion. Two potential mechanisms by which PRAF1 mutations affect ACTH secretion and localization are: either the enhanced Dexras1/PRAF1 interaction inhibits the PRAF1/Rab3A/VAMP2 interaction, or since PRAF1 mutations are known to affect interactions with SNARE complex proteins, [18,19] this may be the mechanism by which ACTH secretion is affected. Another potential mechanism might be that processing of proopiomelanocortin (POMC), the precursor to ACTH, is inhibited.

II. LITERATURE REVIEW

Cushing's Disease: An Example of HPA Axis Dysregulation

Cushing's disease is a medical condition characterized by excess secretion of glucocorticoids that has devastating, potentially fatal, effects. In approximately 85% of human and canine spontaneous Cushing's syndrome patients, the excess cortisol is a result of excess ACTH release from a pituitary adenoma. This is accompanied by a raised threshold for glucocorticoid negative feedback at the pituitary.[20,21] Since cortisol has numerous physiological effects, the clinical manifestations of Cushing's syndrome are diverse and include obesity, glaucoma, osteoporosis and muscle atrophy, as well as the more serious and life-threatening problems of hypertension, immunosuppression and blood hypercoagulability.[20,22] Seventy-one percent of human Cushing's patients interviewed in one study reported that the disease "greatly" affected their life and 20% said it affected their life "a lot."[23]

Many studies examining regulation of the HPA axis have focused on the positive control of the system, identifying the neural inputs to hypothalamic stimulatory centers, the mechanism by which hypothalamic peptides stimulate ACTH secretion, and the adrenocortical release of glucocorticoids. Corticotrophs, however, serve a central integrative function, balancing the level of stimulatory input (usually of hypothalamic origin) with the amount of inhibitory signal (glucocorticoid feedback) to determine the ultimate and appropriate amount of ACTH output. A precise determination of the

mechanism governing feedback inhibition may, therefore, lead to a better understanding of the genesis of disorders in the HPA axis such as Cushing's disease.

There are many treatments for Cushing's disease, including partial or total hypophysectomy, pituitary irradiation, and drug therapies.[24-26] However, each of these may lead to serious complications including severe morbidity and mortality. This emphasizes the necessity for developing a new treatment approach for Cushing's disease. Molecular-based approaches have been used to treat many other diseases, including leukemia, melanoma, colon cancer, lung cancer, and pituitary neoplasia.[27-35] However, in order to produce an effective molecular-based treatment, it is first necessary to identify potential targets and assess the viability of those targets.

To my knowledge, only one study has evaluated a molecular-based treatment for Cushing's disease.[36] The study was performed *in vitro* in cells isolated from areas of corticotrophic adenoma and hyperplasia found in a single patient. Liposome-coated antisense oligonucleotides against the first 25 amino acid of POMC, which correspond to ACTH, reduced ACTH secretion by >90%. However, follow up *in vivo* studies have yet to be reported. Since ACTH excess is common to all lesions producing pituitary-dependent Cushing's disease, an effective treatment should address this common problem. In order to do this, it is important to understand how normal corticotrophs function.

The HPA Axis and Negative Feedback

The HPA axis is responsible for regulating the secretion of glucocorticoid hormones from the adrenal cortex. Both physiological and psychological stresses induce

the hypothalamus to release corticotrophin-releasing hormone (CRH) into the hypophysial-portal system, which delivers blood, nutrients, and hypothalamic hormones to the anterior pituitary. Stimulation of the pituitary by CRH results in the release of adrenocorticotropic hormone (ACTH) into the general circulatory system. In the adrenal glands, ACTH stimulates the secretion of cortisol into the bloodstream. The presence of cortisol in the bloodstream provides feedback that inhibits further release of CRH and ACTH and, consequently, cortisol secretion decreases. Because the end product, cortisol, provides a limiting mechanism to inhibit further hypothalamic and pituitary secretion of CRH and ACTH, respectively, the HPA axis is classified as a negative feedback system.

Cortisol-mediated inhibition of pituitary secretion of ACTH is normally classified in two different ways, depending on whether the system is *in vitro* or *in vivo*. *In vivo* there are 3 time frames. The fast response occurs within seconds to minutes of glucocorticoid exposure and is activated in response to rising glucocorticoid levels.[6] The intermediate response occurs within 0.5 hours, but the mechanism is unclear.[6] The slow response takes hours to days and is due to an inhibition of POMC gene transcription which results in a decrease in ACTH synthesis.[6] *In vitro*, the response may be early or delayed. The fast and intermediate responses are both considered early responses because there is virtually no difference between them.[8,37,38] Therefore, for the purpose of this discussion, fast and intermediate responses will be referred to as the intermediate time frame of feedback.

ACTH Production in Corticotrophs

CRH has a stimulatory effect on ACTH secretion, whereas glucocorticoids have an inhibitory effect. The actions of these 2 factors result in cyclic levels of systemic ACTH and cortisol. This section will focus on the stimulatory side of the equation, primarily CRH and the production of ACTH.

In addition to stimulating the regulated release of ACTH from corticotrophs, CRH, a 41- amino acid peptide hormone, induces the synthesis of pro-opiomelanocortin (POMC), the 31 kDa precursor of ACTH and many other biologically active proteins. The idea that ACTH could have a precursor molecule was first proposed in 1971.[39] While researching a case of ectopic ACTH syndrome resulting from a human thymic tumor, Yalow and Berson identified a high molecular weight molecule that was immunoreactive but biologically inactive. Treating this molecule with trypsin released biologically active ACTH. This study triggered the search for an ACTH precursor, or prohormone.[39]

The studies in which POMC was identified and cloned were conducted in AtT-20 cells, a mouse corticotroph tumor cell line. Pulse-chase studies using labeled amino acids were fundamental to discovering that POMC generates not only ATCH, but also β–lipotrophin (LPH) and β–endorphins.[40,41] POMC contains 8 pairs and 1 quadruplet of basic amino acid that act as potential cleavage sites. Initial processing of POMC results in the production of N-terminal peptide (NT), joining peptide (JP), ACTH, and β–LPH.[42,43] NT is further cleaved into γ–melanocyte-stimulating hormones (MSH), ACTH is cleaved into α–MSH and corticotrophin-like intermediate lobe peptide (CLIP), and β–LPH is cleaved into β–MSH and the β–endorphins.[44] How much POMC is

cleaved is determined by the function of the end-product and by the tissue in which the product is expressed. The end products also undergo chemical modifications including glycosylation, amidation, phosphorylation, acetylation, and sulphation. Some of these changes alter the function of the peptide and are therefore cell-specific.

Before POMC can be cleaved into biologically active products, the gene must first be induced, the mRNA processed, and the nascent polypeptide directed into the regulated secretory pathway. In response to stress, CRH induces POMC expression.[45] CRH binds specifically to CRH receptors, which are G-protein-receptors, on corticotrophs [4,5] and initiates the cyclic adenosine monophosphate (cAMP) signaling pathway by activating adenylate cyclase (AC). AC converts adenosine triphosphate (ATP) into cAMP.[2] Elevation of cAMP occurs in a time frame analogous to ACTH secretion in response to stress.[46] Further, ACTH concentrations increase in proportion to CRH dosage[47] and this relationship is not affected by phosphodiesterase inhibitors, suggesting that the increase in AC activity is the likely cause of the elevation in cAMP.[46]

Protein kinase A (PKA) is activated by cAMP[47] and is associated with calcium influx into the cell.[2,48] Protein kinase A inhibitor (PKI) introduced into AtT-20 cells blocks intracellular calcium elevation.[49] PKI also inhibits ACTH release in response to CRH stimulation.[50,51] Phorbol ester stimulation of ACTH release is not blocked by PKI,[51]and phorbol esters act through the protein kinase C second messenger system rather than PKA.[51,52] Therefore, PKA must be involved in CRH-induced ACTH secretion. PKA targets the cAMP Response Element Binding Protein (CREB) which, once phosphorylated by PKA, increases the transcription of cAMP target genes, one of which is POMC.

POMC is also produced in non-pituitary tissues. In the brain, POMC is produced in the arcuate nucleus and is cleaved into cerebral β–endorphins and αMSH, both of which have biological functions in the brain.[53-55] The placenta also produces POMC, although here a biological function has yet to be identified.[56,57] Finally, keratinocytes, melanocytes, and dermal endothelial cells express POMC and MSHs, suggesting that skin regulates its own pigmentation.[58-60]

In humans, pituitary POMC expression occurs only in corticotrophs, whereas other mammals also have an intermediate lobe that contains POMC-expressing melanotrophs. In corticotrophs, mature POMC mRNA is translated into prePOMC protein. The nascent polypeptide is then translocated through the membrane of the rough endoplasmic reticulum (RER), where the signal peptide is cleaved.[61]

Following translation, the nascent polypeptide must be directed into the secretory pathway via translocation into the Golgi complex. Amino acids 1-26 of nascent POMC have been identified as the critical secretory pathway signal residues.[62] This region contains a sorting motif containing Asp_{10}, Leu_{11}, Glu_{14}, and Leu_{18} and is denoted as DLEL.[61] The structure is stabilized by 2 disulfide bridges in a conformation that is critical for binding to carboxypeptidase E (CPE), a regulated secretory pathway sorting receptor, and this motif does not appear to be cell specific. [61,63,64] In addition, glycosylation of POMC occurs as it travels through the Golgi complex.[65,66]

So far, 2 functions for CPE have been identified: 1) membrane-bound 55 kDa CPE sorts proteins into the regulated secretory pathway; and 2) cytosolic 53 kDa CPE cleaves basic residues from the C-terminus of peptides.[67,68] Interaction between membrane-bound CPE and the sorting signal of POMC results in packaging of both into

immature secretory granules.[67] Once CPE and POMC are packaged into the secretory granule, CPE undergoes autocleavage which removes the membrane binding domain and results in the 53 kDa enzymatically active form.[68] This form cleaves the sorting signal from POMC.[68]

POMC is next cleaved between ACTH and β–MSH to yield a 27 kDa ACTH precursor (pre-ACTH) and β–MSH.[69] This is the first step in producing mature ACTH, although, there is some dispute as to whether or not this cleavage occurs before or after POMC is packaged into acidifying secretory granules.[69-71] In 1987, Tooze et al. determined that at least 25-30% of POMC is packaged into secretory vesicles prior to being cleaved into ACTH and β–MSH, and that unprocessed POMC was located at the cell periphery.[69] These researchers theorized that sorting of POMC into secretory granules prior to cleavage is the most likely interpretation and suggested that this conclusion was supported by the finding that all 3 pituitary-based cleavage products are present simultaneously in secretory granules of AtT-20s.[69,72] In addition, research involving prohormone convertase 1 (PC1), the enzyme that cleaves POMC into ACTH and β–MSH in corticotrophs, suggests that in AtT-20 cells POMC is packaged into secretory granules prior to processing.[73-78] PC1 is most active when the pH is between 5.0 and 6.5, as is the case in acidifying secretory granules.[77,78] As the pH of the Golgi cisternae is neutral, PC1, if present, may not be active.

In contrast, Schnabel et al. suggested that cleavage of ACTH from POMC via PC1 begins in the trans-most Golgi complex. In their study they used antisera that only recognized POMC cleavage products and antisera against unprocessed POMC. Since POMC cleavage products were found in the trans-most regions of the Golgi complex,

they concluded that cleavage of ACTH from POMC occurred prior to packaging into secretory granules.[70] In support of this research, when chloroquine, a weak base that dissipates pH gradients in organelles, is added to AtT-20 cells POMC processing is not affected. Since, in this study, an acidic environment was not absolutely necessary for PC1 cleavage activity, it was proposed that PC1, if present, could be active in the Golgi complex.[79]

In an attempt to determine whether or not PC1 is present in the Golgi complex and therefore determine the timing of ACTH cleavage from POMC, Tanaka et al. performed a study to determine the localization of unprocessed POMC, JP, and PC1.[80] Using immunofluoresence and immunogold electron microscopy, they localized PC1 to the perinuclear region and the tips of cellular processes, JP to secretory granules and cellular processes, and POMC to both Golgi cisternae, where condensing granules form, and secretory granules. In addition, 3-[2,4-dinitroanilino]-3'amino-N-methylpropylamine (DAMP) was used to determine the pH of intact AtT-20 cells. The Golgi complex had a neutral pH whereas the pH of secretory granules ranged from 5.2 to 7.0, with lower granular acidity correlating with POMC positive granules near the Golgi and higher acidity with JP positive granules near the tips of cellular processes. Since PC1 was not found in the Golgi cisternae, it appeared unlikely that cleavage of ACTH from POMC began in the Golgi complex. Thus, Tanaka et al. suggest that in AtT-20 cells POMC processing occurs mainly in acidifying secretory granules.[81]

Rab3A and VAMP2

Over 63 different mammalian Rab proteins exist, however, most are restricted to specialized cell types.[82] Rab function is restricted by: 1) localization of each Rab to a specific subcellular compartment, and 2) involvement in a specific transport step. Rabs act as molecular switches, cycling between an inactive GDP-bound and active GTP-bound states.[82] These changes in activity relate to reversible associations between Rabs and their target membranes. Both the GDP/GTP switch and the membrane association/dissociation cycle are critical for the proper functioning of Rab proteins. Hence, to be fully active, a Rab protein must be both GTP-bound and membrane-associated. Cycling of Rabs through GDP/GTP and membrane bound/unbound states allows for both spatial and temporal control of Rab activity and several factors are involved. Rabs are delivered to their target membranes by a Rab-GDP dissociation inhibitor (RabGDI), where they are activated by specific guanine nucleotide exchange factors (GEFs). Once activated, GTP-bound Rabs recruit effector molecules to the membrane. GTP hydrolysis returns Rabs to an inactive state. GDP-bound Rabs are extracted from the membrane by RabGDI, via formation of cytosolic complexes. Rabs undergo multiple cycles of RabGDI-mediated membrane delivery and extraction. The mechanisms by which Rabs regulate other proteins are not fully understood.

Vesicles traveling through the secretory pathway must accomplish several steps, including budding, targeting, docking, and fusion. Soluble N-ethylmaleimide-sensitive factor attachment protein (SNAP) receptors (SNARE) are known to regulate vesicle fusion.[83] Synaptobrevins, also known as vesicle-associated membrane proteins (VAMPs), associate with syntaxin and SNAP-25, both of which are target membrane

proteins, to comprise a core complex whose formation is essential for membrane fusion.[84] Rab effector proteins either interact directly with VAMPs or recruit other SNARE regulators.[85-89] VAMP2, a member of the VAMP/synaptobrevin family, cycles between an active and inactive state, which is regulated by Rab3A. [18,90] Activation VAMP2 is necessary for interaction with syntaxin, and to induce membrane fusion.[85] Syntaxin, SNAP-25, synaptotagmin, and VAMP2 form a stable complex in order to facilitate vesicle docking and fusion with the plasma membrane.[91-93]

The function of Rab3A may be to inhibit random exocytosis. In several cell types, Ca^{2+}-dependent exocytosis is inhibited by Rab3A overexpression.[94-97] As with all Rabs, Rab3A cycles between a vesicle-bound GTP form and a cytosolic GDP form.[98] Upon stimulation via calcium influx, Rab3A is hydrolyzed and dissociates from vesicles.[98] In fact, hydrolysis may be a rate limiting step in exocytosis.[99] However, calcium influx is not enough to induce release of Rab3A from vesicles, suggesting that other regulatory proteins are involved with Rab3A recycling.[99] Indeed, Rab3A recycling is dependent upon association GDI, but other regulatory proteins may also be involved.[100]

Inhibition of ACTH Secretion in the Intermediate Time Frame

Studies have revealed how CRH stimulates the release of ACTH and that glucocorticoids inhibit ACTH release, although the precise point(s) of inhibition in the intermediate time frame has not yet been identified. Stimulation of type II glucocorticoid receptors in corticotrophs appears to initiate feedback.[101] With regard to the intermediate time frame, neither basal secretion of ACTH nor ACTH synthesis is affected.[37] Since basal secretion of ACTH is not affected in the intermediate time frame, Keller-Wood and Dallman suggest that the total amount of ACTH stored at the plasma membrane and the

releasable pool of ACTH are unaffected by glucocorticoid-induced inhibition.[6] Indeed, the intracellular pool of ACTH is not diminished by up to 9 hours of pretreatment with Dexamethasone (Dex) nor does up to 4 hours of pretreatment affect either total protein synthesis or ACTH synthesis.[37]

Several studies have been conducted to determine the step or steps in stimulated ACTH secretion that might be inhibited. The first step that might be inhibited is the interaction between CRH and the CRH receptor, since glucocorticoids down-regulate the cell surface expression of the CRH receptor. However, in AtT-20 cells, receptor depletion does not begin until 4-6 hours after glucocorticoid exposure while intermediate feedback begins after as little as 30 min and only half of the receptors were depleted after 30 hours.[102] Further, complete suppression of ACTH secretion occurs within 24 hours of glucocorticoid exposure.[102] Finally, a 3 week incubation of AtT-20 cells with Dex reduces CRH receptor expression to a small percentage of its original amount without affecting the ability of glucocorticoids to suppress stimulated ACTH secretion.[102] Last, Dex does not inhibit secretagogue binding.[37] Thus, glucocorticoid-mediated inhibition of stimulated ACTH release in the intermediate time frame occurs at a site further along the secretion pathway than the point of CRH/CRH receptor interaction.[102]

As mentioned previously, interaction of CRH with its receptor activates AC which then converts ATP into cAMP. Either of these steps could be a target of glucocorticoids in the intermediate time frame. However, although, oxytocin, phorbol esters, maitotoxin, and potassium chloride stimulate ACTH secretion in corticotrophs through non-cAMP mediated pathways, Dex inhibits ACTH secretion in response to

these compounds.[49,50,103] Thus, Dex must inhibit ACTH secretion either at a site downstream from AC and cAMP or independently of AC and cAMP.[104]

As calcium influx is necessary for stimulated secretion, it is possible that inhibition of ACTH secretion may result from any inhibition of the calcium influx into a cell. Indeed, membrane depolarization, calcium channel agonists, and potassium channel antagonists antagonize the early inhibition of stimulated ACTH secretion. [103,105-108] [37,109,109-111,111] Furthermore, in AtT-20 cells high conductance Ca^{2+} -activated K^{+} -channels (BK-channels) must be inhibited by PKA in order for stimulated ACTH secretion to occur.[112] In addition, Dex prevents PKA-induced BK-channel inhibition, but other inhibitors of BK-channels overcome Dex-mediated inhibition of stimulated ACTH secretion.[112] In contrast, in rat anterior pituitary cell cultures glucocorticoids are still able to inhibit stimulated ACTH secretion in the presence of BK-channel blockade. However, since in rat pituitary cell cultures membrane depolarization via high concentrations of extracellular KCl is able to significantly diminish corticosteroid inhibition to a level similar to that in AtT-20 cells, glucocorticoid inhibition may be mediated by changes in the cell membrane potential.[113]

Since calcium influx is necessary for stimulated ACTH secretion, glucocorticoids may act through calcium channel blockade. However, BayK8644, a calcium channel agonist, failed to induce ACTH secretion in rat pituitary cell cultures that had been pre-treated with Dex.[113] In addition, Dex inhibits the ability of CRH, potassium chloride, and maitotoxin to stimulate ACTH secretion without affecting intracellular calcium concentrations.[48] Further, oxytocin-stimulated ACTH secretion in AtT-20 cells is inhibited by pre-incubation with corticosterone without interfering with oxytocin-induced

changes in free cytosolic calcium.[114] Therefore, the blockade of calcium influx via calcium channels does not appear to be the mechanism in glucocorticoid-induced inhibition of ACTH secretion.

Other studies suggest that glucocorticoid-mediated inhibition of ACTH secretion occurs later in the secretion pathway, i.e. at the plasma membrane. Filamentous actin (F-actin) may produce a "barrier" at the plasma membrane that prevents ACTH secretion. In support if this suggestion, in chromaffin and mast cells glucocorticoid treatment stabilizes the actin cytoskeleton, as evidenced by a thickening of F-actin bundles and an inability of cytochalasin to disrupt the F-actin bundles.[115-118] In addition, as revealed by freeze-etch electron microscopy of AtT-20 cells, F-actin forms a 3-dimensional web-like matrix near the membrane which seems to hold secretory vesicles near the plasma membrane.[115] Further, in AtT-20 cells, glucocorticoids are also able to stabilize F-actin as well as inhibit ACTH release and both of these effects are overcome by exposing AtT-20 cells to high concentrations of the actin-disruptors cytochalasin B and D.[119] Thus, the links that hold secretory granules may need to be disrupted in order for stimulated release of ACTH to occur.[119]

Finally, protein synthesis is required for intermediate feedback. Dex-induced inhibition of ACTH secretion is blocked by dichlorobenzimidazole ribofuranoside (DRB), an inhibitor of mRNA transcription,[48,104,113] actinomycin,[120] cyclohexamide,[8,37] or puromycin,[8,104] which are inhibitors of protein synthesis. Therefore, synthesis of a protein is necessary but what this protein is or how it acts is unknown. However, it is plausible that this protein acts to stabilize protein-protein interactions within the F-actin

network, or affects membrane polarization, or inhibits SNARE complex formation thereby inhibiting stimulated ACTH release.

Dexras1

Dexras1 was first identified using differential display by Kemppainen and Behrend in a screen designed to identify proteins whose expression is induced in AtT-20 cells by glucocorticoid exposure.[15] Dex treatment of AtT-20 cells resulted in rapid up-regulation of an mRNA encoding a novel protein structurally similar to the GTP-binding proteins of the Ras superfamily. It was therefore named Dexras1 [15] and is the prototypic member of the Ras-related intermediate molecular weight, basic GTP-binding proteins (G proteins). This group includes Dexras1, the activator of G protein signaling 1 (AGS1),[121] the Ras homologue enriched in striatum (Rhes),[122] tumor endothelial marker 2 (TEM-2),[123] and *Drosophila* Dexras and is characterized by highly basic net isoelectric points and molecular weights that fall between those of other Ras family members and the heterotrimeric G protein α subunits.[16]

The predicted protein structure of Dexras1 contains several regions that are conserved throughout the Ras superfamily, including a carboxy-terminal CAAX region, G1 and G3 (phosphate binding loops that interact with GTP/GDP) and G2, G4 and G5 (guanine base binding loops).[15,16,124] The G2 region is thought to be involved in effector binding.[125] The carboxy-terminal region of Ras proteins is typically prenylated, a process that is necessary for membrane localization for many Ras proteins[126], and Dexras1 is predicted to undergo farnesylation.[15] The predicted length of Dexras1 is 280 residues,[15] longer than most Ras proteins, which generally consist of between 180 and 220 residues.

BLAST analysis of the predicted protein sequence showed that Dexras1 has the highest homology with human Rap-2b.[15]

Human and mouse Dexras1 are similar in size, sequence, and organ expression, although mouse Dexras1 protein is one amino acid shorter than the human protein.[124,127] At the nucleotide and amino acid level, human and murine Dexras1 cDNA are 90% and 97% homologous, respectively. Northern blot analysis of human tissues has shown that while Dexras1 is found in many tissues, expression concentrations are highest in the pituitary gland.[127] In addition to human tissues, Dexras1 expression is stimulated by glucocorticoids in murine heart, kidney, and liver, and in HT-1080 cells, a human fibrosarcoma cell line.[124,128]

The human homologue of Dexras1 was identified using a yeast-based screen designed to detect proteins that activate heterotrimeric G-proteins in situations where the receptor is unoccupied. The gene was named activator of G-protein signaling (AGS1) and its protein product is thought to regulate heterotrimeric G-proteins.[121] Gβγ release from Giα is enhanced via direct interaction between Dexras1/AGS1 and Gi *in vitro* in mammalian cells and Dexras1/AGS1 preferentially binds GTP *in vivo*.[112,121,129-131] Conformational changes in Dexras1/AGS1 associated with guanine nucleotide binding and/or hydrolysis may unmask the regions that facilitate GDP release from Gα.[121] Alternatively, Dexras1/AGS1 may act to disrupt G-protein-coupled receptor signaling complexes.[132,133]

Even though the exact role of Dexras1 has not been elucidated, there is evidence that it may function in intermediate feedback. G proteins are active in a variety of cell regulatory processes including regulation of cell proliferation,[134] gene transcription,[135]

mRNA stability and translation,[136-138] cytoskeletal organization,[139,140] peptide trafficking,[141,142] and secretion.[143,144] In addition, Graham et al. hypothesized that glucocorticoid-dependent inhibition of secretion from the cAMP-stimulated pathway is regulated by Dexras1 and predicted that inhibition of cAMP-stimulated peptide hormone secretion could be achieved by over-expression of a wild-type or constitutively active Dexras1 protein in the absence of glucocorticoids. Indeed, cAMP-stimulated human growth hormone secretion was significantly attenuated in the presence of a constitutively active Dexras1 mutant, suggesting that endogenous Dexras1 may participate in specific aspects of glucocorticoid-dependent signal transduction.

However, with regard to intermediate feedback, the Dexras1/Gi interaction does not seem to play a role. When CRH binds its receptor, the Gs subunit is activated resulting in stimulated ACTH secretion.[2,4,5] Dexras1 interacts with Giα, but not Gs.[121] In addition, Dex is able to block secretion in response to several other ACTH secretagogues, namely oxytocin, phorbol 12-myristate 13 acetate, maitotoxin, and KCl; the former 2 activate PKC and the latter 2 activate voltage-gated calcium channels.[6,103] Consequently, it is unlikely that Dexras1 blocks stimulated secretion via its interaction with Giα.

Indirect evidence indicates that Dexras1 is involved in intermediate feedback. In AtT-20 cells, Dexras1 mRNA increased significantly after 30 minutes of Dex exposure, peaked at 2 hours, and then declined rapidly. It was still above baseline 8 hours post-exposure, but by 24 hours post-exposure the concentrations of Dexras1 mRNA had returned to baseline.[16,128] This pattern of expression corresponds to the intermediate time frame for feedback in corticotrophs.

Unpublished studies also support a potential role for Dexras1 in intermediate feedback. Since Dexras1 has a proposed prenylation site, and prenylation is necessary for Ras protein function, ACTH secretion and negative feedback were assessed in wild-type AtT-20 cells and in AtT-20 cells stably transfected with either Flag-tagged full-length Dexras1 or Flag-tagged prenylation-deficient Dexras1 (R. Kemppainen, unpublished data, 1998). CRH stimulated ACTH secretion from wild-type cells, and stimulated secretion was significantly inhibited by Dex pretreatment. However, in cells transfected with full-length Dexras1, CRH stimulated ACTH secretion to a level similar to wild-type cells that had been pretreated with Dex. In addition, unlike the wild-type cells, Dex pretreatment of these stable transfectants did not reduce CRH-stimulated ACTH secretion. Cells transfected with prenylation-deficient Dexras1 had CRH-stimulated secretion and a response to Dex similar to that of wild-type cells (R. Kemppainen, unpublished data, 1998). Thus, it seems likely that Dexras1 protein is involved in the Dex-induced inhibition of ACTH secretion and prenylation may be required.

In addition to the heterotrimeric G-protein signaling pathway, Dexras1 is involved in other signaling pathways. Dexras1 stimulates Elk1 transcription in transfected HEK293 and COS-7 cells via stimulation of ERK-1/2. In HEK293 and in AtT-20 cells, c-Jun is also activated by Dexras1.[16,145-147] Phosphorylation of c-Jun is typically via the mitogen-activated protein kinase (MAPK) family, as is ERK1/2. Whether or not Dexras1 interacts with Elk1 or c-Jun has not been determined; nor has the effect that these 2 proteins might have on intermediate feedback.

Dexras1 may be an effector of nitric oxide signaling via interactions with CAPON.[148] CAPON associates with neuronal nitric oxide synthase (nNOS) and may aid in targeting of nNOS.[146] Prenatal alcohol exposure is associated with restricted brain growth that is precipitated by decreases in nNOS,[149-151] possibly due to altered Dexras1 expression.[148] However, to my knowledge a potential role of nitric oxide in pituitary feedback has not been investigated.

In summation, Dexras1 is involved in intermediate feedback and most likely acts late in the ACTH secretion signaling pathway, but precisely where and how have yet to be determined. Two mechanisms of inhibition have been proposed: (1) Dexras1 interacts with cytoskeletal elements or proteins to stabilize the cytoskeleton, and/or (2) Dexras1 interacts with exocytotic proteins to inhibit secretion.[128]

Prenylated Rab Acceptor Domain Family Member 1 (PRAF1)

PRAF1 was isolated and characterized during studies designed to define the role of Rabs in vesicle trafficking.[18] Using a yeast two-hybrid screen with Rab3A as bait, Martincic et al. identified a rat protein that interacts with both Rab3A and VAMP2 and named it "prenylated Rab acceptor 1" or PRA1.[18] Bucci and colleagues utilized a yeast two-hybrid screen using canine Rab7 for bait and a human brain cDNA library to look for Rab interactors.[152] As a result, human PRA1 was isolated and characterized. The gene for murine PRA1 has also been cloned and sequenced.[153] Since there are multiple prenylated Rab acceptor domain family members,[154] in 2006, the HUGO Gene Nomenclature Committee determined that prenylated Rab acceptor domain family

member 1 (PRAF1) would be the official name for PRA1. PRAF1 has also been called prenylin and, in yeast, Yip3.

The exact function of PRAF1 is unknown; however, it localizes to the Golgi complex, post-Golgi vesicles, synaptic vesicles, and endosomes, and may play a role in vesicular trafficking throughout the cell.[19,155-158] The cellular location of PRAF1 was detected by indirect immunoflourescence, fusion of PRAF1 to Green Fluorescent Protein, and co-localization studies with the Golgi marker mannosidase II.[153] Fenster et al. conducted a flotation assay with lysed synaptosomes and found that PRAF1 is associated with synaptic vesicles.[156] PRAF1 was associated with Rab5-containing early endosomes and Rab9-containing late endosomes and has been shown to incorporate these 2 Rabs into liposomes *in vitro*.[158]

Rat, mouse, and human PRAF1 are similar in size, sequence, and organ expression. Human PRAF1 is a 185-residue protein with an estimated molecular weight of 20.7 kDa.[18] Both rat and mouse PRAF1 are approximately 21 kDa.[18,152,153] The deduced rat and human PRAF1 proteins are 95% homologous at the amino acid level.[152] With the exception of two amino acids, mouse PRAF1 protein is identical to that of rats.[152] Both mouse and rat PRAF1 are expressed in placenta, pituitary gland, kidney, testis, skeletal muscle, liver, lung, spleen, brain, heart, and stomach.[18,152,153] The Golgi membrane insertion signal may be located in the carboxy-terminus of PRAF1, as deletion of up to 90 amino acids from the amino-terminus failed to abolish Golgi complex localization, whereas deletion of the last ten amino acids of the carboxy-terminus did.[153] Residues 176-179 comprise a DXEE motif necessary for exit from the endoplasmic

reticulum (ER).[159,160] The DXEE region is also acidic and mutations that neutralize this region result in the retention of PRAF1 in the ER.[155]

Structuraly, PRAF1 has hydrophilic amino-terminus (residues 1-78), linker region (residues 113-131), and relatively short carboxy-terminus (residues 166-185).[161] Two hydrophobic domains exist, HD1 (residues 79-112) and HD2 (residues 132-165), each of which has two transmembrane regions (TM 1-4) that induce a fold in their hydrophobic domain.[161] As a result, when PRAF1 is associated with the Golgi complex all three hydrophilic regions are expected to be found in the cytoplasm, where they are able to interact with other cytoplasmic proteins. Virtually none of PRAF1 extends into the lumen of the Golgi complex (Figure 1).[161]

Because very little of the protein is actually in the lumen of the Golgi complex, the PRAF1/Golgi membrane association may be unstable.[161] In fact, PRAF1 is found in both the cytosolic (15%) and membrane portions (85%) in cellular fractionation studies in which PRAF1 was overexpressed.[162] Whether as much as 15% of PRAF1 is cytosolic at physiologic concentration is unknown. The carboxy-terminus (residues 166-185) is critical for ER to Golgi transport of PRAF1 and may function in maintaining PRAF1 in a soluble state, as deletion of this region causes PRAF1 to act as an integral membrane protein.[162,163] Thus, PRAF1, while predominantly membrane bound, may be able to associate and disassociate from membranes.

PRAF1 may, in general, mediate vesicular trafficking through interactions with Rab proteins,[157] which are GTPases responsible for regulation of transport vesicle docking and fusion.[141,142] Rab proteins need to be activated (GTP-bound) and prenylated for PRAF1 binding to occur, and PRAF1 probably acts as a Rab regulator, since a

complete Ras effector domain is not required for interaction.[18,152,157] In addition to interacting with Rab3A, PRAF1 also binds to Rab4A and B, Rab5A and C, Rab 6, Rab7, Rab 17, and Rab 22.[86,164-169] Rab4 proteins regulate endosomal fusion, while Rab5 proteins control clathrin-mediated endocytosis at the plasma membrane, guide early endosome transport along microtubules, and are necessary for docking and fusion of transport vesicles.[164-168] Rab7 governs the late endocytic pathway.[169] Given this apparent lack of Rab specificity, the current theory is that PRAF1 association with Rab proteins is limited by the sub-cellular localization of PRAF1, i.e. PRAF1 regulates the Rabs present in the organelles with which PRAF1 interacts. In yeast, the exact function of Yip3, the yeast homologue of PRAF1, is unknown. However, PRAF1/Yip3 interacts with the yeast proteins Yip1p, Ypt1p, and Ypt31p, the homologues of the mammalian proteins Rab1, Rab1A, and Rab11, respectively, which localize to the Golgi complex and are involved in intra-Golgi vesicle trafficking.[158,170]

When associated with the Golgi complex, PRAF1 may be necessary for vesicle formation as well as vesicle trafficking, possibly by interacting with SNARE proteins. To determine the effect of PRAF1 mutations on cellular morphology and vesicle trafficking, Chinese hamster ovary cells (CHO) were stably transfected with mutated forms of PRAF1. Different cellular phenotypes were created which were grouped into classes based on their Golgi morphology.[19] In CHO cells, wild type PRAF1 mainly localized to the Golgi complex but class A cells retained mutant PRAF1 in the ER and had inhibited intra-Golgi transport. PRAF1 mutants localized to a condensed Golgi complex in class B cells, suggesting an inhibition of anterograde transport from the Golgi complex. Class C cells exhibited Golgi complex and ER localization of PRAF1 mutants,

along with the development of tubular structures that emanated from the Golgi complex. The cellular phenotype also correlated with altered Rab3A/VAMP2 interactions; PRAF1 mutations that resulted in class A or C phenotypes had decreased binding with Rab3A and VAMP2, whereas in class B cells, Rab3A and VAMP2 had increased binding to mutant PRAF1. Finally, all cells were co-transfected with PRAF1 and vesicular stomatitis virus glycoprotein (VSVG), a viral envelope protein. VSVG transport to the plasma membrane was either greatly diminished or completely inhibited in all cells transfected with mutant PRAF1 and insertion of VSVG into the plasma membrane did not occur in any cells transfected with a PRAF1 mutant, suggesting that functional PRAF1 is necessary for vesicular trafficking within the cell and fusion of transport vesicles with the plasma membrane.[19]

There are several theories as to how PRAF1 and Rabs interact. First, PRAF1 may bind to prenylated regions of the Rabs and aid in GTPase trafficking by masking Rab hydrophobic regions.[157] Second, PRAF1 may assist in the packaging of GTPases into vesicles for transport to the plasma membrane by acting as a GTPase sorting protein in the Golgi complex and may shuttle Ras proteins to the plasma membrane.[157] Third, since PRAF1 associates with guanine nucleotide dissociation inhibitor (GDI), disrupts endosomal Rab/GDI complexes, and promotes Rab membrane association, PRAF1 may serve as a GDI-displacement factor for Rab proteins. However, this role is most likely utilized only when Rabs are tightly bound to GDI.[142,158]

As discussed earlier, Rab3A and VAMP2 interact, resulting in the activation of VAMP2, a necessary prerequisite for SNARE complex formation and exocytosis.[85] As assessed by a yeast two-hybrid assay, PRAF1 interacts with Rab3A and VAMP2, and

Rab3A and VAMP2 share the same 2 interaction sites on PRAF1 (residues 30-54 and 175-185).[18] Therefore, Martincic et al. proposed a mechanism for the interaction of VAMP2, Rab3A, and PRAF1, suggesting that in an unstimulated cell, PRAF1 is bound to VAMP2.[18] Upon stimulation Rab3A, which is an activator of VAMP2, binds to PRAF1, releasing and activating VAMP2. Once activated, VAMP2 interacts with syntaxin, another exocytotic protein, resulting in fusion of the plasma and vesicular membranes and exocytosis (Figure 2).[18] Further, they proposed 2 possible mechanisms for the PRAF1/Rab3A/VAMP2 interaction. First, since Rab3A and VAMP2 bind to the same segments of PRAF1, Rab3A and VAMP2 may compete for the same binding site on PRAF1.[18] Indeed, when the molar concentration of Rab3A is twice that of PRAF1, Rab3A disrupts the formation of a VAMP2/PRAF1 complex.[162] Alternatively, a PRAF1/Rab3A interaction may cause a conformational change, resulting in a decreased affinity of PRAF1 for VAMP2.[162]

On the other hand, a Rab3A/PRAF1 interaction may act to inhibit Rab3A activation and thus prevent premature VAMP2 activation. Full-length PRAF1 inhibits the interaction between guanine dinucleotide protein dissociation inhibitor (GDI) and Rab3A, as shown by extraction studies using PC12 microsomal membranes.[162] The membrane vs. cytosolic localization of Rab3A is dependent upon the opposing action of GDI and PRAF1, with PRAF1 favoring membrane association.[162] Thus, PRAF1 may regulate the interactions of Rab proteins with proteins in the SNARE complex, primarily with VAMP2, possibly by inhibiting recycling of Rab3A.[162]

Additional evidence suggests that PRAF1 may play a role in SNARE complex formation. PRAF1 and Piccolo, a component of the presynaptic cytoskeletal matrix, co-

localize and interact in the active zone of neurons.[156] Since Piccolo contains a proline–rich region that may interact with SH3 domains and a PDZ region that interacts with other proteins, two theories for a PRAF1/Piccolo interaction have been proposed: (1) Piccolo is part of a scaffold that aids in PRAF1 and VAMP2/t-SNARE interactions; and/or (2) PRAF1 transiently associates with Piccolo, unmasking Rab3A and/or VAMP2 to allow an interaction to occur and SNARE complexes to form.[156]

PRAF1 interacts with other Ras proteins including Ha-Ras, a GTP binding protein with significant sequence homology to Dexras1. Ha-Ras interacts with PRAF1 in a prenylation-dependant manner and co-localizes with PRAF1 to the Golgi complex.[157] Another Ras protein, RhoA, interacts with PRAF1 and also co-localizes with PRAF1 to the Golgi complex. Finally, the Ras proteins TC21, and Rap1A (in mammalian cells, but not yeast) also bind to PRAF1.[157] These findings provide further evidence that PRAF1 may function in the regulation of small GTPases.

PRAF1 Interacts with Viral Proteins

PRAF1 interacts with several viral proteins and may have protective effects against viral infection. In addition to potential functions in vesicle formation and trafficking, PRAF1 may play a role in protecting cells from Epstein-Barr virus, a member of the Herpes viral family. Both rat and human PRAF1 interact with the Epstein-Barr virus early gene protein BHRF1, a structural and functional homologue of the anti-apoptotic protein Bcl-2.[171] BHRF1 localizes to mitochondria, where it inhibits apoptosis signals from external stimuli and cell-signaling factors.[172,173] The regions of PRAF1 that are important for interaction with BHRF1 are residues 30-53, which have a high arginine

content, and residues 164-185, which have charged acidic glutamates in the sequence.[171] As these are the same regions that interact with Rab3A and VAMP2, BHRF1 may compete with these two proteins for binding to PRAF1.[18,171] Full-length PRAF1 and PRAF1 (30-185) both decrease the anti-apoptotic activity of BHRF1, whereas PRAF1 (1-164) cannot bind BHRF1 and does not decrease the anti-apoptotic activity.[171] Since PRAF1 localizes to the Golgi complex, it may act to sequester BHRF1 to the Golgi complex so that apoptosis cannot be inhibited.[171]

PRAF1 also interacts with the conserved cytoplasmic domain (CD) of lentiviral envelope glycoproteins (gp41 CD) from human, simian, feline, and bovine immunodeficiency viruses and equine infectious anemia viruses.[174] Since gp41 CD interacts with multiple host factors, it may function in the regulation of viral replication. Since the exact role of PRAF1 is still unknown, the function of a PRAF1/gp41 CD interaction can only be the subject of speculation. However, based on PRAF1 localization and interactions with other proteins, a few possible roles for PRAF1/retroviral glycoprotein interaction can be proposed. First, PRAF1 may direct nascent envelope glycoproteins to appropriate Golgi compartments, thus facilitating post-translational modification of the proteins, such as glycosylation, cleavage and palmitoylation.[174] Second, a gp41 CD/PRAF1 interaction may serve to sort the glycoprotein into transport vesicles bound for the basolateral plasma membrane, targeted via a tyrosine-based sequence in the gp41 CD segment.[174,175] Third, PRAF1 may regulate fusion of transport vesicles containing viral proteins with the plasma membrane via an interaction with SNARE proteins.[176] Fusion of transport vesicles containing viral proteins with host plasma membranes converts part of the plasma membrane into viral

envelope and creates a target for the naked virion.[175,177,178] In polarized cells infected with a retrovirus, envelope glycoprotein is inserted into the basolateral membrane, the site of virion release.[179]

Finally, a yeast two-hybrid screen of a CV1 (African green monkey kidney) cell cDNA library identified VP4 as a PRAF1 interactor.[180] VP4, a 776-residue rotaviral spike protein, is known to play a role in cell attachment, penetration, hemagglutination, and virulence[181-183] and is required for infectivity.[184,185] VP4 may also aid in budding of single-shelled capsids into the lumen of the ER, where maturation into double-shelled capsids probably occurs.[186,187]

The function of a VP4/PRAF1 interaction is unknown. Since VP4 does not associate with the Golgi complex but does associate with Golgi-derived lipid rafts on post-Golgi vesicles,[188,189] PRAF1 may recruit VP4 to lipid rafts.[180] Localization of VP4 with lipid rafts aids in viral assembly and cell surface expression of VP4.[190] Taken together, these data suggest that a VP4/PRAF1 association augments rotaviral assembly and cell surface expression of VP4, possibly via PRAF1-mediated recruitment of VP4 to areas of viral assembly localized to lipid rafts.[180]

Dexras1/PRAF1 Interaction

Glucocorticoid-induced inhibition of ACTH secretion during intermediate feedback may be mediated via Dexras1, PRAF1, Rab3A, and VAMP2 interactions. Based upon the work of Martincic et al., it seems likely that in corticotrophs Dexras1 interacts with PRAF1, thus preventing a VAMP2/Rab3A/PRAF1 interaction. As a result, activation of VAMP2 would not occur, VAMP2 and syntaxin would not be able to

interact, and ACTH secretion would be blocked. Since Dexras1 does not bind to the same sites on PRA1 as do Rab3A and VAMP2, Dexras1 inhibition of Rab3A/VAMP2/PRA1 interaction may be indirect, i.e. binding of Dexras1 to PRAF1 blocks Rab3A/VAMP2 access to their binding sites on PRAF1. Alternately, PRAF1/Dexras1 interaction may result in a conformational change in PRAF1 which results in an inability of Rab3A or VAMP2 to recognize their binding sites on PRAF1.

It is also possible that Dexras1 inhibits POMC processing, thereby reducing the amount of ACTH available for stimulated secretion. Inhibition of processing could be accomplished by Dexras1 inhibiting PRAF1/Rab3A interaction in the Golgi complex, resulting in diminished vesicle formation and trafficking through the Golgi. As a consequence, POMC would not be processed into ACTH. Therefore, the hypothesis examined in this study is that PRAF1 mutations will abolish the interaction with Dexras1, thus affecting not only PRAF1 localization, but also the localization and secretion of ACTH and the processing of POMC.

In order to test this hypothesis, the research reported in this dissertation first generated mutated and truncated versions of PRAF1: PRAF(54-175), PRAF(54-112), PRAF(N70T), PRAF(Y73A), and PRAF(V161A). The mutated genes were then stably transfected into AtT-20 cells. Finally, the effects of the mutations on Golgi morphology, PRAF1/Dexras1 interaction, and the ACTH secretion pathway were assessed via confocal microscopy, Western blotting, yeast two-hybrid, RT PCR, cell function assays, and ACTH IRMA. In addition, wild type (WT) AtT-20s and AtT-20s stably-transfected with empty vector (3X) were also assessed in terms of their Golgi morphology and the ACTH secretion pathway.

AtT-20 Cells as a Model for Glucocorticoid Inhibition

Isolation of corticotroph cells is difficult because they 1) represent a minority in whole pituitary cultures or dispersed cell cultures, 2) attempts to enrich cell cultures for corticotrophs have proved less than optimal, and 3) almost all the cells in the pituitary respond to glucocorticoids.[5,191] Therefore, an alternative cell type that could be grown in culture would be beneficial. Woods et al. evaluated the usefulness of AtT-20 cells, an ACTH-secreting mouse pituitary tumor cell line that produces and secretes large amounts of ACTH, for investigating early glucocorticoid inhibition. Using the secretagogues CRH and phorbol esters to examine ACTH secretion, Woods et al. determined that glucocorticoid-mediated inhibition of stimulated ACTH release was reliable in AtT-20 cells. Furthermore, the synthetic glucocorticoid, Dex, inhibited CRH-induced ACTH release. Within 45 min, stimulated release was inhibited and strongly (80-90%) suppressed at 2 hours. In addition, as in normal corticotrophs ACTH secretion from AtT-20 cells increases in response to CRH in a dose-dependant manner,[192] and glucocorticoid inhibition of ACTH secretion in AtT-20 cells has an onset of action within minutes of glucocorticoid exposure, is mediated by type II glucocorticoid receptors, and requires mRNA and protein synthesis.[37,48,104,192]

AtT-20 cells do differ from normal pituitary corticotroph cell in a few aspects. Unlike normal corticotrophs, VP treatment of AtT-20 cells does not result in ACTH secretion, even though AtT-20 cells express a VP receptor.[193] In addition, within 30 sec, AtT-20 cells rapidly become refractory to somatostatin stimulation.[194] Further, AtT20 cells seem to have spontaneous electrical activity whereas in normal corticotrophs there

are either no spontaneous calcium influxes, or the fluxes are rhythmic in nature.[195,196] However, although these cells do not quite function as normal cells, AtT-20 cells can serve as an acceptable model for intermediate feedback.

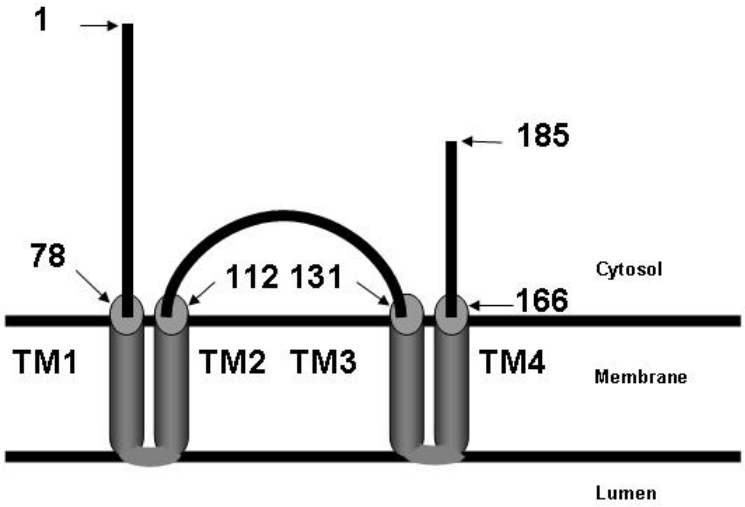

Figure 1. Membrane topology of PRAF1 and insertion into the Golgi membrane. Numbers refer to amino acids. TM refers to the transmembrane regions (1-4). Hydrophobic regions are residues 78-112 and 131-166. Hydrophilic regions are residues 1-77, 113-130, and 167-185. Adapted from Lin et al.[161]

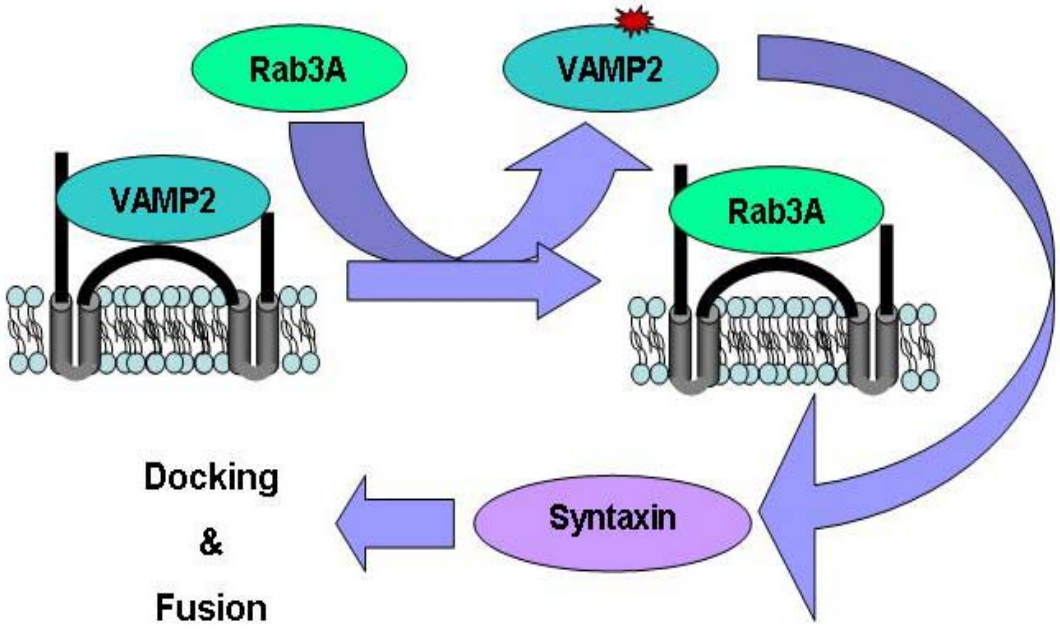

Figure 2. Proposed interaction of Rab3A, VAMP2, and PRAF1. VAMP2 is bound to PRAF1 (grey and black), which is inserted into the transport vesicle membrane and oriented such that the hydrophilic regions of PRAF1 and VAMP2 protein are in the cytoplasm. When Rab3A associates with the transport vesicle membrane, the PRAF1/VAMP2/Rab3A interaction disrupts PRAF1/VAMP2 binding. As a result, VAMP2 is activated (represented by a red star) and interacts with syntaxin. Docking and fusion of the transport vesicle with the target membrane then follows.[20]

III. MATERIALS AND METHODS

Cell Culture Protocol

Wild type AtT-20 cells (ATCC, Manassas, VA) were maintained in Dulbecco's Modified Eagle's Medium (DMEM) supplemented with L-glutamine, 4500 mg glucose/L, 10% (v/v) fetal calf serum (Life Technologies, Gaithersburg, MD), 5 mM Hepes (Invitrogen, Carlsbad, CA), and antibiotic/antimycotic (final concentration: 100 units/mL penicillin, 100 ug/mL streptomycin, 0.25 ug/mL amphotericin B, Invitrogen). Stably transfected AtT-20 cells were maintained in DMEM supplemented with L-glutamine, 4500 mg glucose/L, 5 mM Hepes, and 10% (v/v) fetal calf serum and Geneticin (0.8 mg/mL, Life Technologies) (10%DMEM). All cell types were grown in a humidified atmosphere of 5% CO_2/95% air at 37 ^oC.

Generation and Cloning of PRAF1 Mutants

Subcloning techniques were used to construct the truncated PRAF1 mutant vectors. Full length PRAF1 (FL PRAF1) and the 2 truncated constructs [PRAF(54-175) and PRAF(54-112)] had been previously cloned into the pGAD vector (BD Biosciences Clontech, Palo Alto, CA).[1] The pGAD vector, with inserts, and p3X-Flag-CMV-10 vector (Sigma-Aldrich, St. Louis, MO) were digested with *EcoR1* and *BamH1* (New England Biolabs, Beverly, MA) for 2 hrs at 37^oC. The digested products were separated by electrophoresis on a 1.2% agarose gel. The p3X-Flag-CMV-10 vector and PRAF1 inserts were eluted with the Zymoclean Gel DNA Recovery kit (Zymo Research, Orange,

CA) and then purified with the Zymo DNA Clean and Concentrator kit (Zymo Research) as per the manufacturer's instructions. Each digested insert was ligated with the digested vector (T4 DNA ligase, Promega, Madison, WI) as per the manufacturer's instructions. Ligated vectors were sequenced to confirm that there were no errors.

Three PRAF1 point mutations [PRAF(N70T), PRAF(Y73A), and PRAF(V161A)] were induced using FL PRAF1 in pGAD as a template via PCR and the Quickchange Site-directed Mutagenesis kit (Stratagene) as per the manufacturer's instructions. Primers utilized to introduce the desired point mutations were designed with the Quickchange Primer Design program (Stratagene, LaJolla, CA) (Table 1). PCR parameters were an initial denaturation at 94 ^{o}C for 5 min, followed by 25 cycles of 94^{o}C for 15 sec, 62^{o}C for 30 sec, and 72^{o}C for 60 sec, concluding with a single lengthening step at 72^{o}C for 5 min. The PCR products were digested with *Dpn 1* restriction enzyme for 1 hr at 37^{o}C to remove the template vector. The resulting vectors were sequenced to ensure they had the correct mutations. The mutated PRAF1 constructs were subcloned into the p3X-Flag-CMV-10 vector as above.

Transformation and amplification of PRAF1 constructs. Each PRAF1-containing vector was transformed into DH5α bacterial cells (New England Biolabs) using the DH5α Subcloning efficiency kit (Invitrogen), as per the manufacturer's instructions. Bacteria were plated on imMedia AMP Agar (Invitrogen) for selection, and ampicillin (100 μg/mL) was used in LB media for positive selection during the clonal expansion. Plasmids were recovered with the Zippy Plasmid Miniprep Kit I (Zymo Research).
To create stably-transfected AtT-20 cells, wild type (WT) AtT-20 cells were transfected with 4 μg of p3X-Flag-CMV-7 vector itself or containing the gene for PRAF1, PRAF(54-

112), PRAF(54-175), PRAF(N70T), PRAF(Y73A), or PRAF(V161A) using the LipofectAMINE Plus (Life Technologies) protocol as per the manufacturer's instructions. The cells were transfected at ~ 70% confluence. The day after transfection, trypsin was added (0.15% trypsin in PBS, Invitrogen) followed by 3 mL of 10% DMEM and the cells were triturated. Three mLs of cells were plated onto each of 4 culture dishes (150 x 15 mm Petri dishes) and 27 mL of 10% DMEM was added to each. The medium was replaced with an equal amount of freshly prepared medium the following day.

Ten colonies from each plate were chosen for cloning. Each colony was isolated via a cloning cylinder, 10 μL of 0.15% trypsin was added and the sample was incubated at room temperature for 10 min, after which 200 μL of 10% DMEM was added to the cylinder and triturated 10 times. The medium and cells were then transferred to a 48-well plate. After 6 days, 4 clones with growth rates similar to WT AtT-20 cells were chosen from each plate for transfer to 25 cm^2 flasks. After 2 passages, western blot was performed to ensure that PRAF1 was strongly and equivalently expressed in each stably-transfected cell line.

Yeast Two-Hybrid Assay

For yeast two-hybrid assay, the Matchmaker Two-Hybrid System 3 (Clontech, Mountain View, CA) was used. Dexras1, which had previously been cloned into the pGBKT7 bait vector,[1] and one of the pGAD-PRAF1 construct vectors were co-transformed into the AH109 strain of yeast (Clontech) using 0.5 μg of DNA of each plasmid and the Frozen-EZ Yeast Transformation II kit (Zymo Research) as per the manufacturer's instructions. The appropriate positive and negative controls included

with the kit were also transformed. For interaction analysis, transformed yeast were plated on SD-YW (-trp/leu) plates containing X-α gal (Clontech), SD-YWH (-trp/leu/his), and SD-YWHA (-trp/leu/his/ala) and then incubated at 30°C. The SD-YW was used to ensure that both plasmids had been transformed into the cell. The other 2 deficient media were used to test whether or not interaction was abolished. After 5 days, the number of colonies ≥ 1 mm in diameter and the presence or absence of a color change (indicating β-galactosidase activity) were recorded. Finally, the plates were wrapped in parafilm and stored at 4°C.

Cell Function Assay

Wild-type and stably transfected AtT-20 cells were plated in 48-well plates at a density of 200,000 cells/mL and allowed to grow for 2 days. On the day of the study, the media was changed to DMEM supplemented with 0.1% BSA (DMEM/BSA) and the cells were incubated for 1 hr at 37°C. Media was removed and vehicle (Veh, 100 nM EtOH in DMEM/BSA) or dexamethasone (Dex, 100 nM) were added to the cells, followed by incubation for 2 hrs. Subsequently, media was again removed and Veh, CRH (100 nM, Sigma-Aldrich) or Dex/CRH were added followed by incubation for 1 hr. Following the final treatment, the media was collected from each well and centrifuged at 12,000 X g for 10min, and the supernatant stored until analysis at -20°C. The cells were then washed briefly in 0.5 mL RIA buffer [0.1% Triton X-100, 250 KIU/mL Trasylol, 16.84 mg/mL $Na_2HPO_4 \cdot 7H_2O$, 4.74 mg/mL $Na_2EDTA \cdot 2H_2O$, 0.2 mg/mL NaN_3, pH 7.4)] and lysed for 30 min at 4°C in 0.2 mL RIA buffer. The lysates were transferred to 1.5 mL tubes and centrifuged at 14,000 x g for 10 min. The supernatant was removed and

stored at -20°C. Functional studies on all cell types were repeated 5 times; in each experiment, treatments were repeated in 4 wells.

In both media and cell lysates, ACTH concentration was determined using an ACTH IRMA Assay kit (Scantibodies Laboratory, Santee, CA) as per the manufacturer's directions. There were 2 antibodies in the kit. The first recognized ACTH(1-16) and the second recognized ACTH(24-39). Therefore, only mature ACTH was recognized in this assay. To normalize the data for variations in cell number between wells and replicates, the ACTH concentration in a sample was divided by the total protein concentration.

Western Blot

Western blotting was used to evaluate the relative concentrations of FL PRAF1 and all mutant constructs, plus POMC, pre-ACTH and ACTH in all cell types (n=4). To ensure that the bands detected were the desired proteins, a Western blot was performed where the anti-ACTH and anti-Flag primary antibodies were pre-incubated for 1 hr with ACTH or FLAG-BAP. On each Western blot, a media sample and cell lysate from a single representative well of each cell type was used. For cell lysates, 10 μg of total protein were used whereas for media samples, 100 μg of total protein was loaded. Acetone was added to each sample (4X volume) and the samples were incubated at -20 °C for 1 hr. Following incubation, the protein precipitate was concentrated via centrifugation at 1,100 rpm for 8 min. The supernatant was removed and the pellet was allowed to air dry for 10-15 min. The pellet was resuspended in 15 μL of loading buffer (Tris-tricine with 0.05% β-mercaptoethanol diluted 1:2 in RIA buffer, Biorad) preheated to 95 °C. The proteins were denatured by heating at 95 °C for 5 min. Flag-tagged BAP

protein (Sigma-Aldrich) was used as a positive control in gels loaded with media samples. In the gel used to analyze lysates samples, 10 mg of a 3T3 NIH mouse embryonic cell lysate and 0.0125 mg of synthetic ACTH (combined into 1 sample) served as the positive control. Samples were fractionated on Criterion 10-20%, 28 lane gels (BioRad) and transferred to Immobilon-FL Transfer Membranes (Millipore, Billerica, MA). Membranes were blocked with Odyssey Blocking Buffer (Li-Core Biosciences, Lincoln, NB) diluted 1:1 in PBS (PBS/BB).

PRAF1 constructs were detected in both media and lysate samples using a primary mouse anti-FLAG antibody (1:1,000, Sigma-Aldrich) followed by an immunofluorescent goat anti-mouse secondary antibody (1:20,000 IRDye 800 CW, Li-Cor Biosciences). POMC, pre-ACTH, and ACTH were detected with a rabbit anti-ACTH primary antibody (1:400, generous gift from R. Kemppainen) followed by an immunofluorescent anti-rabbit secondary antibody (1:20,000 IRDye 700 DX, Li-Cor Biosciences). The rabbit anti-ACTH antibody detected all ACTH-containing peptides including ACTH, pre-ACTH, and POMC. All antibodies were diluted in PBS/BB supplemented with 0.1% triton X-100. Membrane washes were performed between each antibody incubation for 3 x 5 min. The blots were incubated first in the rabbit anti-ACTH antibody for 1 hr, followed by the mouse anti-FLAG antibody for 1 hr, and finally incubated in a mix of the secondary antibodies for 1 hr.

The Odyssey Infrared Imaging System (Li-Cor Biosciences) was utilized for image evaluation. The anti-rabbit secondary antibody was detected in the 700 channel and the anti-mouse antibody in the 800 channel. Bands were detected using the Odyssey software with integrated intensity and top/bottom background reduction. For

standardization and statistical analysis, the intensity of the experimental bands was divided by the intensity of the appropriate control band (calculated integrated intensity). The control band for the ACTH-containing peptide image was the 30 kDa POMC band from the lysate gel control lane (700 channel) and the control band for the PRAF1 image was the 31 kDa PRAF1 band from the media gel control lane (800 channel).

RT PCR

AtT-20 cells were grown in 25 cm^2 flasks until approximately 70% confluent. The medium was aspirated from each flask, 500 μL of trypsin was added and the cells were incubated at 37^oC for 10-15 min. Cells were pelleted via centrifugation at 300 x g for 5 min and the supernatant was removed. RNA was extracted using the RNeasy Kit (Qiagen, Valencia, CA) as per manufacturer's instructions. cDNA was synthesized using the iScript 1st strand synthesis kit using 1 μg of total RNA (Bio-Rad, Hercules, CA) and real-time PCR was performed on a myIQ real-time PCR detection instrument using SYBR green supermix (Bio-Rad). The gene specific primers used in real-time PCR were: mouse pro-opiomelanocortin (POMC, Accession # NM_008895) sense 5'-cggccccaggaacagcagcagt and antisense, 5'-catctccccacaccgcctcttcct. Polymerase chain reaction using this primer pair with cDNA from AtT-20 cells yielded a single product of the expected size; sequence analysis confirmed its identity. The thermocycler program was as follows: an initial denaturation at 94°C for 2 min, followed by 35 cycles of 94°C for 15 sec, 60°C for 30 sec and 68°C for 1 min. Melt curve analysis showed the presence of 1 amplicon and no primer dimerization. PCR efficiency was determined by 10-fold cDNA dilution followed by real-time PCR. Data were normalized to the housekeeping

genes glyceraldehyde 3-phosphate dehydrogenase (GAPDH, Accession # NM_008084) (sense 5'-gaggccggtgctgagtatgtcgtg, antisense 5'-tcggcagaaggggcggagat) and 2'-5' oligoadenylate synthetase-like 2 (Oasl2, Accession # NM_011854 (sense 5'-cagcgagcgagggatgttcag, antisense 5'-gcgcagttcccctccaaagtt. Expression of GAPDH and Oasl2 in AtT-20 cells were not affected by short-term (exposure duration 2 hr or less) treatment with dexamethasone or corticotropin-releasing factor (unpublished findings). Data were analyzed using a modification of the delta delta Ct method as described by Vandesompele, et. al.[197]

Confocal Microscopy

Wild-type and stably transfected AtT-20 cells were plated at 200,000 cells/mL on 8-well Permanox Lab-Tek chamber slides with covers (Nalg Nunc International, Rochester, NY). Two hundred μL of cells was added to each well, and cells were grown for 2 days.

On the day of the imaging, media was removed, and the cells were rinsed briefly in 500 μL PBS. Cells were fixed in 10% paraformaldehyde in PBS for 15 min and permeabilized in 0.2%Triton X-100 for 5 min. Image-it (Fisher Scientific) was added for 30 min for blocking and enhancement of immunofluoresence. Cells were then incubated for 1 hr in the primary antibody mix, which consisted of chicken anti-ACTH (1:400, Abcam, Cambridge, MA), rabbit anti-giantin (1:1,000, Covance, Berkeley, CA), and mouse anti-Flag (1:700, Sigma-Aldrich) antibodies. The cells were washed 3 x 5 min in PBS supplemented with 3% normal goat serum (PBS/NGS, Sigma-Aldrich) and incubated for 1 hr in the secondary antibody mix, which consisted of Alexa-Fluor 488

(goat anti-mouse), Alexa-Fluor 568 (goat anti-rabbit), and Alexa-Fluor 647 (goat anti-chicken) (Molecular Probes, Carlsbad, CA) antibodies, all diluted 1:1,000 in PBS/NGS. To ensure that autofluorescence of AtT-20 cells did not occur, 2 wells underwent the entire immunoflourescence protocol except for the addition of antibodies as a preliminary experiment. In addition, to ensure that cross-reactivity did not occur between the primary antibodies and secondary antibodies from another species, each primary antibody was incubated with each of the secondary antibodies from the non-matching species. Further, each primary antibody was incubated with the AtT-20 cells without a secondary antibody to ensure that the primary antibodies did not autofluoresce. Finally, each secondary antibody was incubated with cells but without a primary antibody to ensure there was not any non-specific interaction between the AtT-20 cells and the secondary antibodies. A BioRad MRC 1024 Confocal Scanning Laser Microscope was used to view the slides and confocal images of triple-labeled cells were obtained via the LaserSharp 2000 software (BioRad). Alexa-Fluors 488, 568 and 647 were excited at 495 nm, 578 nm, and 650 nm and emission wavelengths were collected at 510 nm, 519 nm and 668 nm, respectively.

Statistical Analysis

For cell function studies, the ACTH concentration in the media or lysate was averaged for the 4 wells within a cell type that received the same treatment. The averaged data from all replicates for each treatment and cell type combination were then pooled, and a one-way ANOVA with Bonferroni adjustment for post hoc comparisons was used to compare the amount of ACTH secreted in response to each treatment within a cell type, e.g. the amount of ACTH secreted in response to vehicle, CRH, and

Dex/CRH treatment was compared for WT cells, for 3X cells, etc. In addition, the amount of ACTH secreted in response to vehicle, CRH, and Dex/CRH treatment for a cell type was compared to what was secreted by WT cells. Significance was set at the $p<0.05$ level.

For the Western blot data, the bands from the 700 channel (ACTH) lysate images were used to determine the total concentration of ACTH-containing peptide for each vehicle-treated cell type by combining the calculated integrated intensities for each band within a lane on the lysate image. This total was then compared the same as for the cell function assay, except 4 replicates were pooled (1 for each replicate image). The bands from the lysate images were also used to determine the effects of PRAF1 mutations on POMC processing by comparing ratio of ACTH/POMC, ACTH/pre-ACTH, and pre-ACTH/POMC, again using the calculated integrated intensities with 4 replicates. Since they both represent mature ACTH, the 13 and 6 kDa bands from the 700 channel media images were combined and compared the same as for the ACTH IRMA. Significance was set at the $p<0.05$ level.

For the PRAF1 images (800 channel), the calculated integrated intensities for all bands within a lane on an image were combined. The averaged data from all replicates for each treatment and cell type combination were then pooled, and a one-way ANOVA with Bonferroni adjustment for post hoc comparisons was used to compare the amount of PRAF1 expressed in cell type. Media and lysate images were compared individually. Significance was set at the $p<0.05$ level.

Construct	Forward Primer	Reverse Primer
FL PRAF1	5'-CCCAGACATATGGCG GCCCAGAAGGACCAG-3'	5'-CCCAGAGGATCCTTACA CAGGGTTCCATCTGCAG-3'
PRAF(54-175)	5'-CCCAGAGAATTCATTC TCGCGACCCCGCAATGT GGGA-3'	5'-CCCAGAGGATCCCTATGC AGGGCTCCATCTGGTGGAA GGC-3'
PRAF(54-112)	5'-CCCAGAGAATTCATTC TCGCGACCCCGCAATGT GGGA-3'	5'-CCCAGAGGATCCCAGATA GAGAATGTAACAGGCGCC-3'
PRAF(N70T)	5'-GCGCCTGGTACGCA**C** CGTGGAGTATTAATCAAA -3'	5'-TTTGATTAATACTCCAC**G** GTGCGTACCAGGCGC-3'
PRAF(Y73A)	5'-TGGTACGCAACGTGG AG**GC**TTATCAAAGCAACT ACGTG-3'	5'-CACGTAGTTGCTTTGATAA **GC**CTCCACGTTGCGTACCA-3'
PRAF(V161A)	5'-GAGCCACGCTGG**C**AC TCATAGGCTCC-3'	5'-GGAGCCTATGAGT**G**CCA GCGTGGCTC-3'

Table 1. Primers used to create PRAF1 constructs**.** For the constructs containing point mutations, the specific mutations are in red.

IV. RESULTS

Yeast Two-Hybrid assay

The point mutations introduced into PRAF1 are within the region previously identified as being necessary for interaction with Dexras1.[1] Thus, it is possible that the mutations could alter a Dexras1/PRAF1 interaction. A yeast two-hybrid assay was utilized to assess this possibility. Yeast co-transformed with a vector containing the Dexras1 gene and a vector containing PRAF(N70T), PRAF(Y73A), or PRAF(V161A) grew on complete media, SD-YW, SD-YWH, and SD-YWHA plates and exhibited β-galactosidase activity (n=4, Table 1). The mutations enhanced the interaction, as evidenced by growth on SD-YWHA. In addition, cells transformed with mutant PRAF1 had a consistently darker blue color generated by interaction between Dexras1 and the mutant forms of PRAF1 compared to interaction between Dexras1 and FL (Table 1). Interaction between PRAF(54-175) or PRAF(54-112) with Dexras1 were previously assessed.[1]

Cell Function

In WT AtT-20 cells, CRH stimulates ACTH secretion and dexamethasone (Dex) pre-treatment significantly inhibits CRH-induced ACTH secretion. PRAF1 interacts with Rab3A and VAMP2, proteins involved with vesicle docking and fusion.[18] Mutations in PRAF1 inhibit or abolish interactions with Rab3A and VAMP2.[18] Therefore, PRAF1

mutations could alter the cellular response to CRH and Dex. To determine if this occurs, WT AtT-20 cells and those stably-transfected with 3X, FL and all mutant versions of PRAF1 were assessed for basal ACTH secretion as well as their ability to respond to CRH and Dex.

Basal secretion of mature ACTH was significantly higher in PRAF(54-175), PRAF(54-112), PRAF(N70T), and PRAF(Y73A) than in WT cells (Figure 1). With respect to stimulated secretion, in WT cells, CRH significantly increased ACTH secretion over vehicle treatment ($p<0.001$) and Dex significantly inhibited this response ($p<0.001$), but ACTH secretion was still significantly higher than that from vehicle treated cells ($p=0.002$) (Figure 1). Similar results were obtained with the 3X cells, indicating that transfection did not affect the response to CRH or Dex, as well as in FL stable transfectants (Figure 1). ACTH secretion was not altered by exposure to CRH or CRH/Dex in PRAF(54-175), PRAF(54-112), and PRAF(N70T). In PRAF(Y73A), CRH significantly stimulated ACTH secretion compared to vehicle ($p=0.038$), but Dex did not inhibit CRH-stimulated ACTH secretion. In PRAF(V161A), CRH significantly stimulated ACTH secretion compared to vehicle ($p=0.016$), but this was significantly less than CRH-treated WT cells ($p=0.004$). Contrary to WT cells, however, Dex/CRH treatment induced a significantly higher level of secretion compared to CRH treatment ($p=0.002$).

For cellular ACTH concentrations, no significant difference was detected within a cell type between the 3 treatments. However, in FL, PRAF(54-175), PRAF(54-112), PRAF(Y73A), and PRAF(V161A), the ACTH concentration was significantly lower compared to WT cells for all treatments (Figure 2).

Western Blot

The rabbit anti-ACTH antibody used for the Western blot recognized all ACTH-containing peptides, not just mature ACTH. POMC was identified as a 30 kDa band and pre-ACTH as a doublet at 24-27 kDa. Two forms of ACTH were identified – 13 kDa ACTH and 6 kDa ACTH – depending on the glycosylation pattern (Figure 3). Both 13 and 6 kDa ACTH were detected in cell lysates, but only the 6 kDa form was detected in the media (Figure 3).

The calculated integrated intensity results of the Western blots of media samples reflect the IRMA results with regard to ACTH secretion, i.e. CRH stimulated secretion and Dex inhibited this response in WT, 3X, and FL. PRAF(54-175), PRAF(54-112), and PRAF(N70T) did not respond to CRH. In PRAF(Y73A), CRH stimulated ACTH secretion, however, Dex was not able to inhibit this response. Finally, in PRAF(V161A), CRH stimulated secretion, but Dex/CRH treatment stimulated ACTH secretion even further.

Interestingly, pre-ACTH was secreted by cells stably transfected with any form of PRAF1 but not by WT and 3X cells. The overall concentration of ACTH-containing peptides was not significantly different between cell types. However, the concentration of ACTH significantly decreases in FL, PRAF(54-175), PRAF(54-112), PRAF(Y73A), and PRAF(V161A), suggesting the processing of POMC was affected by the PRAF1 mutations (Figure 3, first table). To assess the processing, the ratios of the standardized integrated values for ACTH to pre-ACTH, ACTH to POMC, and pre-ACTH to POMC were calculated. The pre-ACTH/POMC ratio did not differ significantly between the cell

types. However, the ACTH/POMC and ACTH/pre-ACTH ratios were significantly lower in vehicle treated FL, PRAF(54-175), PRAF(54-112), and PRAF(Y73A) cells compared to WT ($p \leq 0.001$)(Figure 3, second table).

Full-length and mutant PRAF1 constructs were detected in both cell lysates and the media, indicating secretion of PRAF1 from AtT-20 cells. PRAF1 bands were detected at sizes that corresponded to either FL PRAF1 (~21 kDa) or the 2 truncated versions (~10 kDa). PRAF1 was always a single band in the media (Figure 4, top). In the lysates of FL, PRAF(N70T), PRAF(Y73A), and PRAF(V161A), PRAF1 bands appeared as a doublet, whereas in PRAF(54-175) and PRAF(54-112), PRAF1 was a single band (Figure 4, bottom). No statistical difference was detected between cell types for the amount of PRAF1 present in either the media or lysates (Figure 4).

POMC Expression

RT-PCR was used to determine if POMC transcription was altered in stable transfectants compared to WT AtT-20 cells. Cells stably-transfected with FL, PRAF(54-112), and PRAF(Y73A) had an approximately 3 fold increase in POMC mRNA over WT while those transfected with PRAF(54-175) had an approximately 4 fold increase. PRAF(N70T) and PRAF(V161A) had an approximately 6 and 5 fold increase, respectively, in POMC transcription (Table 2).

Confocal Microscopy

In stably transfected CHO cells, PRAF1 mutations affect Golgi morphology, result in altered cytoplasmic distribution of PRAF1 as well as retention of PRAF1 in the

ER and perturb localization of vesicular stomatitis virus glycoprotein (VSVG), a protein used to assess intracellular transport.[19] Therefore, possible effects of PRAF1 mutations on Golgi morphology and ACTH and PRAF1 localization in AtT-20 cells were assessed via confocal microscopy. The location of PRAF1 in WT and 3X cells could not be assessed, as any PRAF1 protein in these cells would not have had a FLAG tag; the primary antibody used was anti-FLAG.

Golgi complex shape, size and position were similar to WT in 3X, indicating that transfection itself does not alter the Golgi complex, as well as in FL cells. Only PRAF(54-175) and PRAF(V161A) had altered Golgi structures. In PRAF(54-175), the Golgi apparatus appeared to be expanded, or stretched, whereas in PRAF(V161A), the Golgi apparatus appeared condensed (Figure 5).

In FL cells, ACTH and PRAF1 co-localized throughout the Golgi complex. In addition, ACTH was detected at the cell periphery and PRAF1 in punctate regions in the cytoplasm. In comparison, all other stably transfected AtT-20 cells had altered ACTH and PRAF1 localization. In PRAF(54-175) and PRAF(54-112), ACTH and PRAF1 were distributed throughout the cytoplasm and in the Golgi complex, but co-localization of these two proteins within the Golgi appeared diminished compared to the FL stable transfectant (Figure 5, merge view). In PRAF(Y73A), there was little to no ACTH in the cytoplasm except immediately adjacent to the Golgi complex, but PRAF1 was distributed throughout the cytoplasm. This was the same pattern for PRAF(N70T), except ACTH was also located at the tips of cellular processes. For both of these mutants, co-localization of ACTH and PRAF1 still occurred mainly in the Golgi complex (Figure 5, merge view). In PRAF(V161A), ACTH and PRAF1 appeared to be scattered throughout

the cytoplasm with multiple areas of co-localization along the cell periphery. In addition, compared to FL, ACTH/PRAF1 co-localization in the Golgi complex appeared diminished and punctate in PRAF(V161A) rather than evenly distributed (Figure 5, merge view).

Dexras1 co-transformant	SD-YW	SD-YWH	SD-YWHA	β-galactosidase activity
FL PRAF1	163 ± 15	109 ± 26		++
PRAF(N70T)	214 ± 28	158 ± 14	68 ± 12	+++
PRAF(Y73A)	287 ± 42	172 ± 27	72 ± 18	+++
PRAF(V161A)	236 ± 23	129 ± 18	56 ± 15	+++

Table 1. PRAF1 point mutations enhanced interaction with Dexras1. The values in the table represent the mean ± the standard deviation from 4 replicate yeast two-hybrid assays. Growth on SD-YW plates signified that both plasmids were present within the yeast. Growth on SD-YWH plates indicated the presence of an interaction between Dexras1 and the PRAF construct. Growth on SD-YWHA suggested the interaction between the 2 proteins is strong. Amount of β-galactosidase activity also gauges interaction strength.

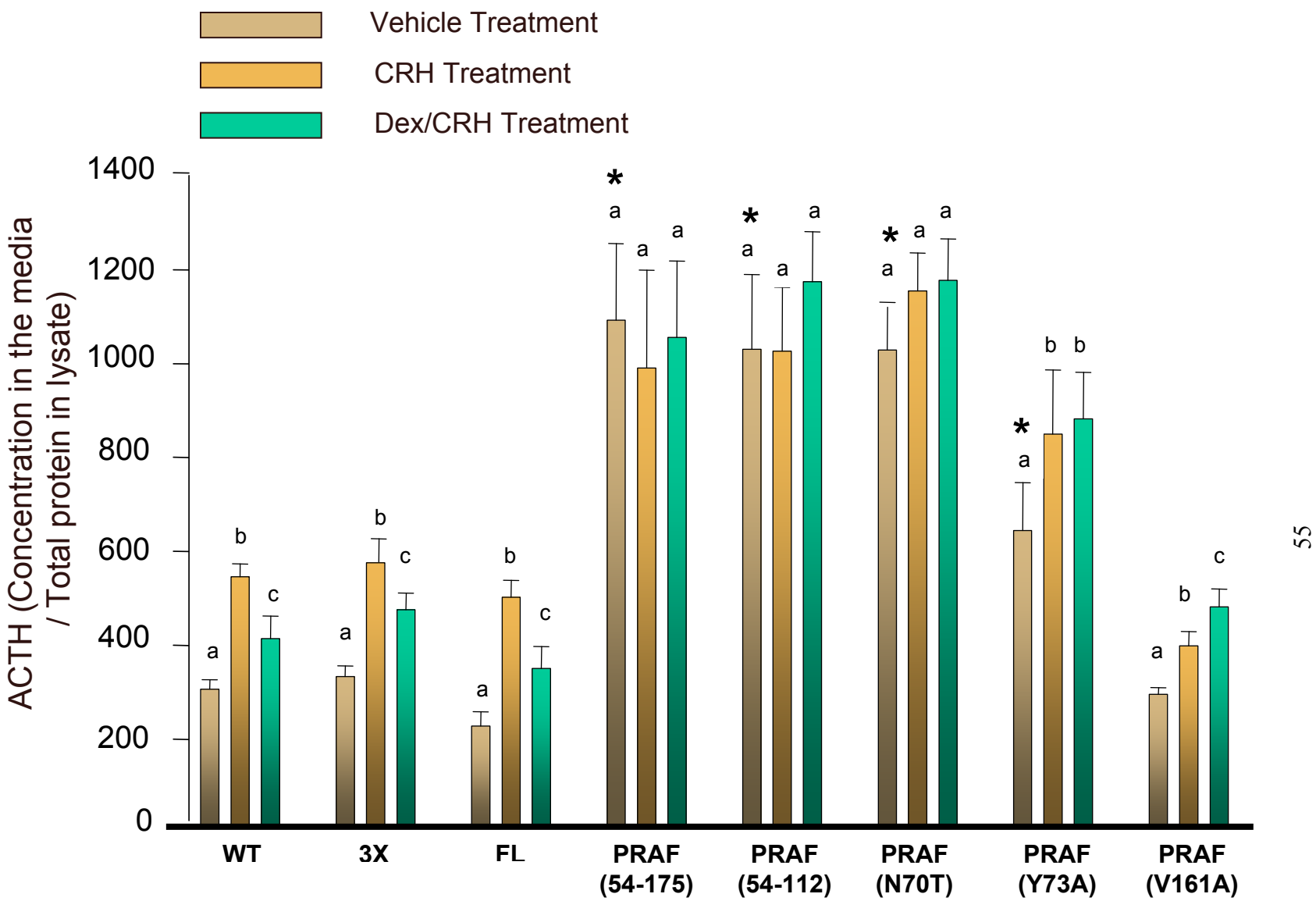
Vehicle Treatment
CRH Treatment
Dex/CRH Treatment
ACTH (Concentration in the media / Total protein in lysate)
1400
1200
1000
800
600
400
200
0
WT
3X
FL
PRAF (54-175)
PRAF (54-112)
PRAF (N70T)
PRAF (Y73A)
PRAF (V161A)

Figure 1. PRAF1 mutations significantly alter basal and stimulated secretion of ACTH in stably transfected AtT-20 cells. ACTH concentration in the media from each well was normalized for total protein concentration in the cell lysate from that well. Bars represent the means of 5 replicates; error bars depict the standard deviation. Within a cell type, different letter above vertical bars indicate significant difference in secretion. * = Significant difference compared to WT for secretion in response to vehicle treatment.

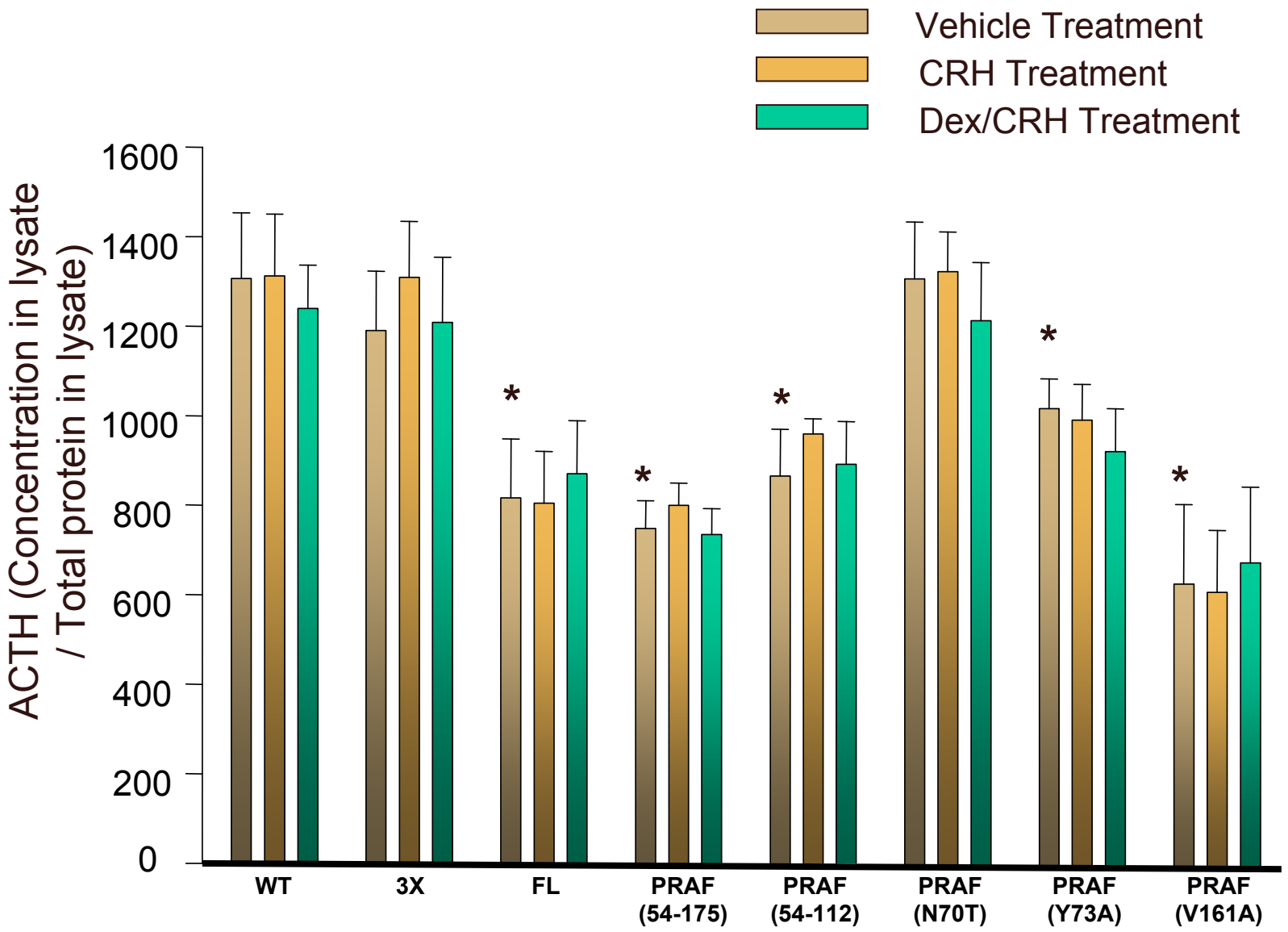
Vehicle Treatment
CRH Treatment
Dex/CRH Treatment
ACTH (Concentration in lysate / Total protein in lysate)
1600
1400
1200
1000
800
600
400
200
0
*
*
*
*
*
WT
3X
FL
PRAF (54-175)
PRAF (54-112)
PRAF (N70T)
PRAF (Y73A)
PRAF (V161A)

Figure 2. PRAF1 mutations significantly decrease the concentration of ACTH in stably-transfected AtT-20 cells. ACTH concentration in the lysate from each well was normalized for total protein concentration in the cell lysate from that well. Bars represent the means of 5 replicates; error bars depict the standard deviation. Treatment with CRH or Dex/CRH treatments did not significantly affect cellular ACTH concentration in any cell type. * = Significant difference compared to WT for cellular content vehicle-treated cells.

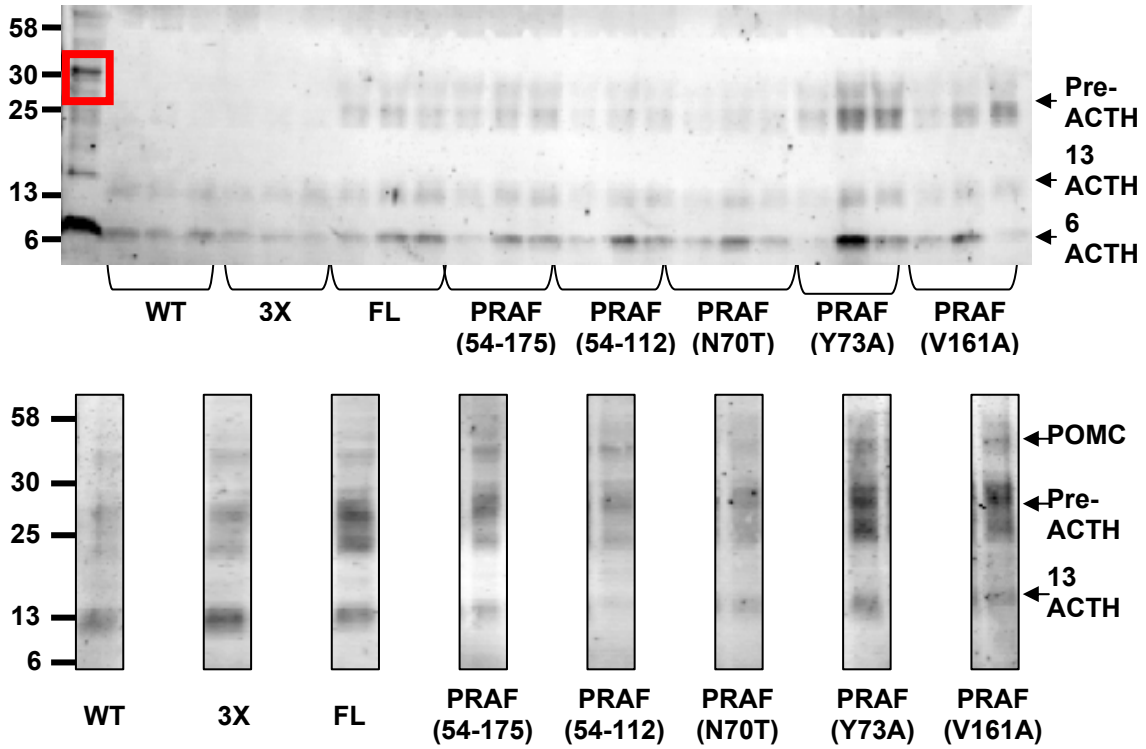

Amount	WT	3X	FL	PRAF (54-175)	PRAF (54-112)	PRAF (N70T)	PRAF (Y73A)	PRAF (V161A)
POMC	1.14± 0.41	1.15± 0.40	1.12± 0.25	1.06± 0.23	1.06± 0.39	1.13± 0.41	1.24± 0.54	1.46± 0.66
pre-ACTH	6.27± 1.77	6.24± 1.44	5.57± 1.17	5.40± 1.10	5.33± 1.53	6.04± 1.24	6.55± 0.25	7.96± 1.76
ACTH	4.51± 1.21	4.32± 0.82	2.34± 0.24*	2.21± 0.31*	2.51± 0.41*	3.46± 0.74	3.22± 0.22*	4.16± 0.96

Ratio	WT	3X	FL	PRAF (54-175)	PRAF (54-112)	PRAF (N70T)	PRAF (Y73A)	PRAF (V161A)
ACTH to pre-ACTH	0.73± 0.05	0.72± 0.07	0.47± 0.08*	0.41± 0.02*	0.48± 0.10*	0.55± 0.10	0.49± 0.03*	0.54± 0.11
Pre-ACTH to POMC	5.92± 1.15	5.80± 0.10	5.24± 1.38	5.23± 0.81	5.11± 0.04	5.60± 0.93	5.52± 0.84	5.99± 1.75
ACTH to POMC	4.26± 0.88	4.11± 0.91	2.22± 0.57*	2.14± 0.26*	2.49± 0.73*	3.06± 0.58	2.67± 0.25*	2.80± 0.09

Figure 3. PRAF1 mutations affect processing of POMC in stably-transfected AtT-20 cells. Representative Western blots for detection of ACTH-containing peptides in media (top) and lysate (bottom) samples are shown (n=4). Brackets denote the 3 lanes within a

cell type; the first lane is media or lysate from vehicle treated cells, the second from CRH treated cells, and the third from Dex/CRH treated cells. The red box encloses the band used to standardize both blots. The values in the first table represent the mean of the concentrations (amount) ± the standard deviation from the Western blots of the lysates of vehicle-treated cells (n=4). * = significantly different from corresponding concentration in WT cells. The values in the second table represent the mean of the ratios ± the standard deviation from Western blots of cell lysates of vehicle-treated cells (n=4). * = significantly different from corresponding ratio in WT cells.

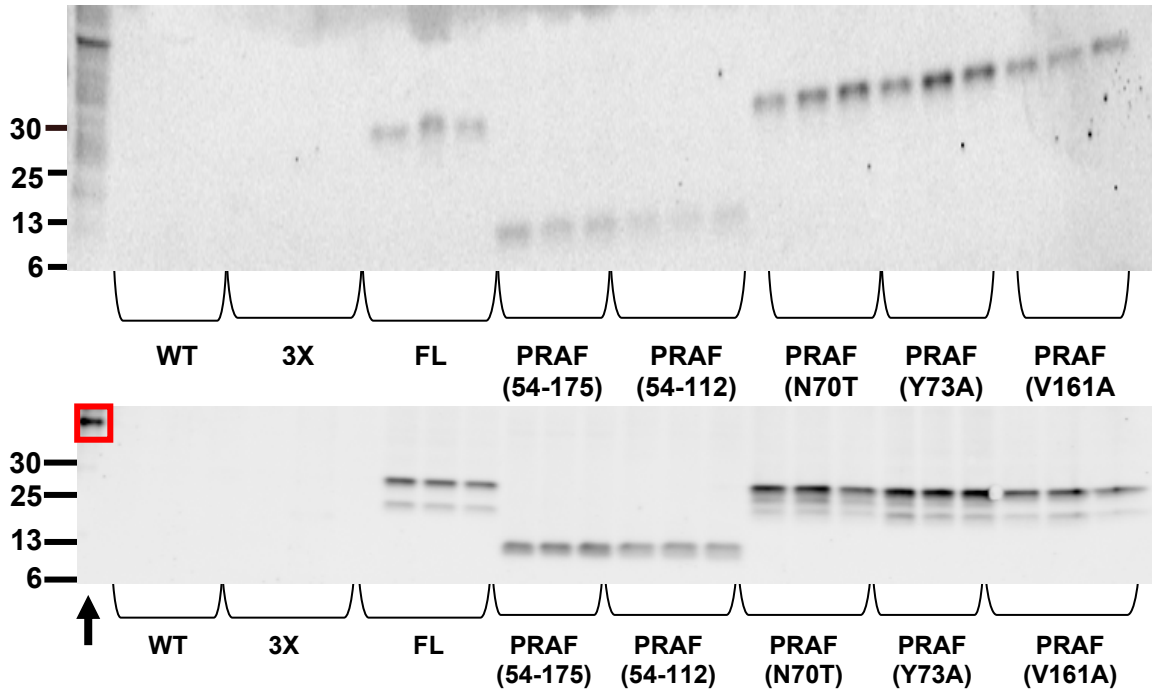

Figure 4. The concentration of PRAF1 was the same in all stable transfectants in both the media and lysates. Representative blots for detection of PRAF1 peptides in media (top) and lysate (bottom) samples are shown (n=4). PRAF1 was detected at sizes that corresponded to either full length PRAF1 (~21 kDa) or the 2 truncated versions (~10 kDa). The FLAG tag on PRAF1 constructs was detected with an anti-FLAG antibody, therefore wild type PRAF1 was not detected in these blots (WT and 3X lanes). See legend of Figure 3 for explanation.

	WT	3X	FL	54-175	54-112	N70T	Y73A	V161A
POMC fold changes	1.00	1.21 ± 0.43	3.13 ± 0.42*	4.37 ± 0.73*	3.28 ± 0.53*	6.17 ± 0.52*	3.37 ± 0.95*	4.84 ± 0.53*

Table 2. PRAF1 mutations affect POMC gene transcription. The relative expression of POMC in the stable transfectants was compared to that of WT AtT-20 cells. Values represent the mean of 3 replicates ± the standard deviation. * = significantly different from WT cells.

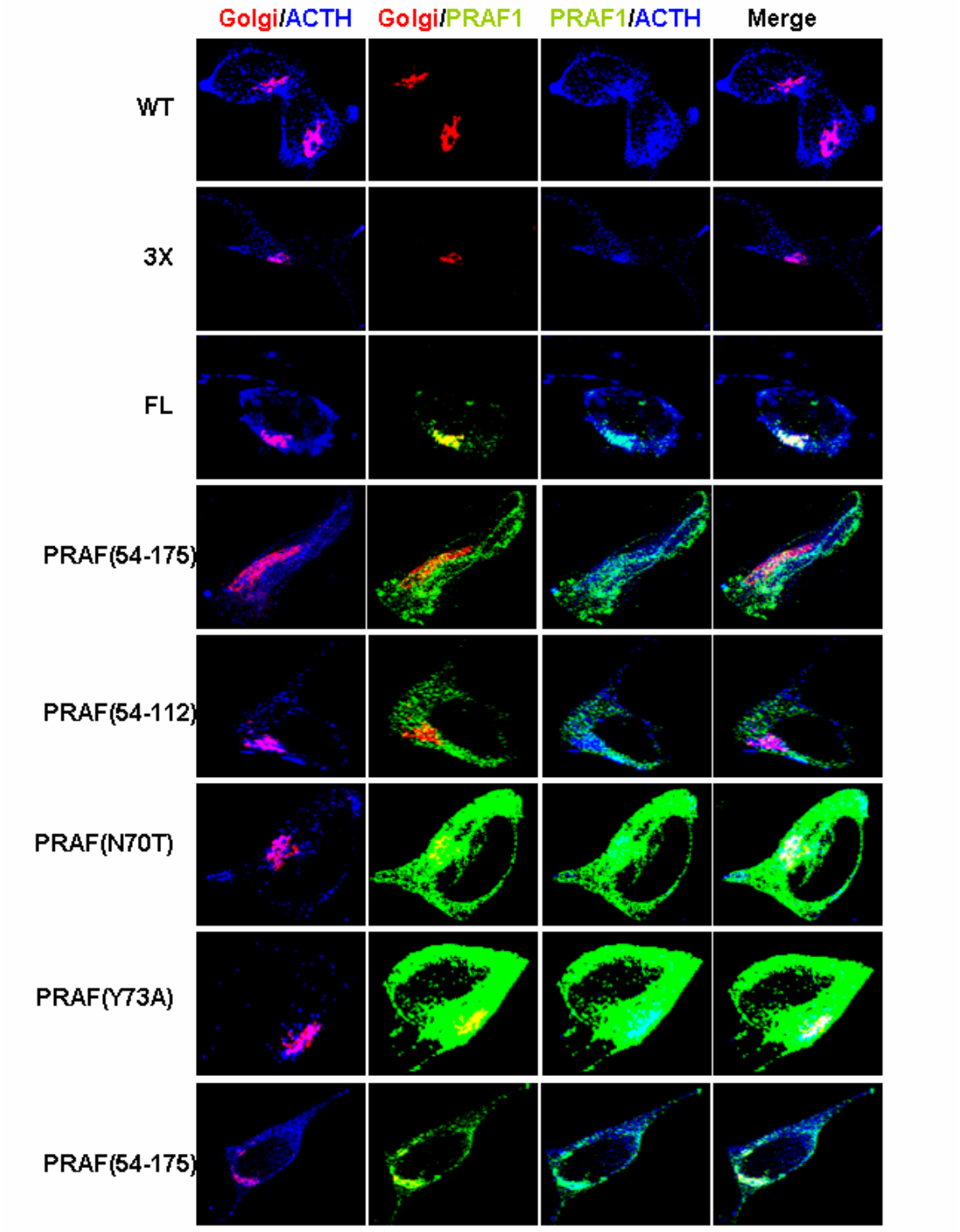
Golgi/ACTH
Golgi/PRAF1
PRAF1/ACTH
Merge
WT
3X
FL
PRAF(54-175)
PRAF(54-112)
PRAF(N70T)
PRAF(Y73A)
PRAF(54-175)

Figure 5. PRAF1 mutations affect Golgi complex morpholgy as well as localization of PRAF1 and ACTH in stably-transfected AtT-20 cells. Individually, the Golgi complex appears red, ACTH appears blue, and FLAG-tagged PRAF1 appears green. Only FLAG-tagged PRAF1 constructs were detected, so PRAF1 was not detected in the WT and 3X cells. Areas of co-localization of the Golgi complex and ACTH appear pink; of the Golgi complex and PRAF1 appear yellow; and of PRAF1 and ACTH appear light blue. In the merge view, co-localization of all 3 appears white.

V. DISCUSSION

How glucocorticoids inhibit stimulated ACTH secretion in the intermediate time frame is unknown. What is known is that protein synthesis is involved, since inhibitors of transcription and/or translation block glucocorticoid-mediated feedback.[8,103,104,120,198] In addition, dexamethasone (Dex) treatment upregulates Dexras1 mRNA expression within 30 minutes of exposure; the expression declines within 8 hours and returns to baseline at 24 hours[15,16], a timeline that would fit a protein involved in the inhibition of stimulated ACTH secretion in the intermediate time frame. Further, constitutively active Dexras1 is associated with inhibition of stimulated hormone secretion in both transiently transfected AtT-20 and Cos-7 cells [16] and stably transfected AtT-20 cells (R.J. Kemppainen, unpublished data). Thus, Dexras1 may play a role in intermediate feedback.

One of the best ways to determine a protein's mechanism of action is to identify proteins with which it interacts. We propose that Dexras1 may be involved in secretion, as Dexras1 interacts with PRAF1.[1,17,199] PRAF1 also interacts with Rab3A and VAMP2 and may link them in the docking and fusion of secretory vesicles since: 1) Rab3A regulates secretion[90,95-100] and inhibits adrenal gland neuroendocrine chromaffin and PC12 cell secretion;[94,200-205]; 2) the PRAF1/VAMP2 interaction is highly specific as PRAF1 does not interact with other members of the VAMP family; 3) Rab3A and VAMP2 are involved in the docking and fusion of regulated secretory vesicles; and 4)

amino acids 30-54 and 175-185 of PRAF1 are essential for interaction with both Rab3A and VAMP2.[18] Further, in Chinese hamster ovary (CHO) cells, PRAF1 mutations that alter Golgi complex morphology and PRAF1 localization also inhibit transport of vesicular stomatitis virus glycoprotein (VSVG), a protein used to assess vesicle transport and protein insertion into the plasma membrane.[19]

We first addressed whether PRAF1 mutations would affect interaction with Dexras1. Since amino acids 54-175 of PRAF1 are necessary for interaction with Dexras1,[1] we sought to determine whether point mutations that occur within this region would affect PRAF1/Dexras1 interaction. Accordingly, 3 PRAF1 point mutations, PRAF(N70T), PRAF(Y73A), and PRAF(V161A), were chosen for this study. All of these point mutations alter the PRAF1/ Rab3A/ VAMP2 interaction in CHO cells.[19] In a yeast two-hybrid assay, truncated PRAF(54-175) and full length (FL) PRAF1 interacted with Dexras1 to a similar degree, whereas truncated PRAF(54-112) did not.[1] PRAF(N70T) abolished interaction with both Rab3A and VAMP2 while PRAF(Y73A) abolished interaction with Rab3A but only diminished that with VAMP2.[19] The third mutation, PRAF(V161A), actually enhanced interactions with Rab3A and VAMP2.[19] In this study, the point mutations affected interaction with Dexras1; however, all 3 PRAF1 point mutations enhanced interaction with Dexras1 compared to FL (Table 1).

The PRAF1/Rab3A/VAMP2 interaction has been proposed to regulate docking, fusion, and secretion.[18,19] Furthermore, in AtT-20 cells stably transfected with Rab3A homologue, o-rab3, ACTH-containing secretory vesicle sequestration was diminished suggesting that Rab3 proteins are involved in secretory vesicle trafficking.[144] The active form of Rab3A, i.e. the GTP-bound form, Rab3A-GTP, may associate with PRAF1 and

block the VAMP2/PRAF1 interaction.[18] Calcium influx into rat hippocampal neurons and bovine chromaffin cells stimulates Rab3A-GTP hydrolysis to Rab-GDP,[99,200] and the same may occur in AtT-20 cells. Rab-GDP would be removed by Rab-GDP dissociation inhibitor (GDI),[141,162,206,207] allowing VAMP2 to interact with PRAF1 and, consequently, VAMP2 to become activated and docking and fusion to follow.[18] After docking and fusion, VAMP2 would dissociate from PRAF1 allowing for Rab-GTP to bind PRAF1 (Figure 1A and B).[18]

We hypothesized that Dexras1 might interfere with a PRAF1/Rab3A/VAMP2 interaction, so we evaluated the effect, if any, of the enhanced PRAF1/Dexras1 interaction on basal, stimulated, and Dex-inhibited ACTH secretion. Wild-type (WT) AtT-20 cells and cells stably transfected with empty 3X-FLAG vector (3X) had a similar level of basal ACTH secretion, response to CRH stimulation, and inhibition by Dex. In WT and 3X stable transfectants, ACTH-containing peptide was detected along the cell periphery and throughout the Golgi complex; ACTH-containing peptide distribution in the cytoplasm was also similar in these 2 types of cells, indicating that stable transfection was not responsible for the observed effects in the other cell lines created.

Our results indicate that an interaction of PRAF1 with VAMP2 may be necessary for CRH-stimulated ACTH secretion in AtT-20 cells, although interaction with Rab3A is not. Cells stably transfected with constructs for PRAF1 mutant proteins that do not interact with VAMP2 – PRAF(54-175), PRAF(54-112) and PRAF(N70T) – did not respond to CRH treatment, while cells transfected with constructs for mutant proteins that do interact with VAMP2 – PRAF(Y73A) and PRAF(V161A) – did (Table 1). Since PRAF(Y73A) protein does not interact with Rab3A, a PRAF1/Rab3A interaction must

not be necessary for stimulated secretion to occur in AtT-20 cells and may be inhibitory. In fact, in AtT-20 cells containing PRAF(V161A), stimulated ACTH secretion was significantly less than in WT cells. The decrease could be due to Rab3A acting as an inhibitor of a PRAF1/VAMP2 interaction,[18] as the interaction between Rab3A and PRAF1(V161A) is enhanced.[19]

Furthermore, our results indicate that a functional PRAF1/Rab3A/VAMP2 interaction may be necessary for Dex-mediated inhibition of stimulated secretion in the intermediate time frame. Unfortunately, Dex-induced inhibition of stimulated secretion was impossible to assess in PRAF(54-175), PRAF(54-112), and PRAF(N70T) stably transfected cells as they did not respond to CRH. However, the mutant protein PRAF(Y73A) interacted strongly with Dexras1 in our study and interacts weakly with VAMP2,[19] but not with Rab3A (Table 1).[19] Stimulated ACTH secretion from cells stably transfected with this mutant was not inhibited by Dex pretreatment (Table 1), possibly indicating that a PRAF1/Rab3A interaction is necessary for Dex-mediated inhibition of CRH-stimulated ACTH secretion. PRAF(V161A) strongly interacts with Rab3A, VAMP2,[19] and, in our study, Dexras1. In cells stably transfected with this mutant, ACTH secretion was significantly increased by CRH. Paradoxically, though, ACTH secretion was further significantly increased by pretreatment with Dex (Table1). The strong PRAF1(V161A)/Rab3A interaction may be a stronger inhibitor of the PRAF1/VAMP2 interaction. However, the enhanced PRAF1(V161A)/Dexras1 interaction may serve to disrupt the PRAF1(V161A)/Rab3A interaction, allowing for a higher rate of Rab3A displacement compared to CRH treatment alone. As a result, VAMP2 activation would occur, and docking, fusion and secretion would follow.

Alternatively, the PRAF1(V161A) protein could be interacting with other proteins resulting in increased secretion in the presence of Dex.

We propose that, via interaction with PRAF1, Dexras1 inhibits stimulated ACTH secretion by adding another step in the regulation of VAMP2 activation. Given that amino acids 54-175 of PRAF1 are necessary for the PRAF1/Dexras1 interaction and these regions are adjacent to those needed to interact with Rab3A and VAMP2,[1] Dexras1 may transiently block Rab3A and VAMP2 access to PRAF1. Dexras1 may block interaction either directly or, since the Dexras1 and Rab3A/VAMP2 interaction sites do not overlap, indirectly by inducing a conformational change in PRAF1 that inhibits interaction with Rab3A and VAMP2. In either case, Dexras1 would need to be removed from PRAF1 for either Rab3A or VAMP2 to interact with PRAF1, and, consequently, when Dexras1 is present, CRH-stimulated ACTH secretion would be slowed (Figure 2). Alternately, Dexras1 may block PRAF1 interaction with Rab3A or VAMP2 in a manner that is not transient. However, the concentration of Dexras1 may not be high enough to interfere with all the vesicles undergoing fusion with the plasma membrane. Determining the relative concentrations of PRAF1, Rab3A, VAMP2, and Dexras1 may help elucidate which, if either, theory is correct.

Another possibility for Dexras1 inhibition of PRAF1/Rab3A/VAMP2 interaction might be that Dexras1 binds Rab3A-bound PRAF1 and prevents GTP hydrolysis. Finally, in HEK293 cells, PRAF1 inhibits the ERK1/2 pathway.[132] Since Dexras1 stimulates ERK1/2 activation[132] and PRAF1 inhibits it, perhaps Dexras1 exerts its effect by blocking PRAF1-mediated inhibition of ERK1/2 activation. However, to our

knowledge, ERK1/2 has not been associated with intermediate feedback, and future studies would need to be performed to elucidate a role for ERK1/2.

Interestingly, FL and mutant PRAF1 proteins were secreted by cells stably transfected with a PRAF1 construct. Since the antibody used to detect PRAF1 was against the FLAG tag of the constructs, wild type PRAF1 was not detected. Therefore, whether wild type PRAF1 is secreted or whether secretion from the stable transfectants is due to PRAF1 overexpression was impossible to determine. To our knowledge, secretion of PRAF1 has not previously been assessed or reported in any cell type.

As trafficking of VSVG, PRAF1 localization, and cellular morphology were disrupted in CHO cells transfected with vectors containing PRAF1 point mutation constructs[19], we hypothesized that PRAF1 mutations would affect ACTH localization and secretion in AtT-20 cells and would alter localization of PRAF1 protein and cellular morphology. Unfortunately, as the primary antibody used to detect PRAF1 was against the FLAG tag of the PRAF1 constructs, the location of PRAF1 in wild type (WT) AtT-20s and AtT-20s stably transfected with empty vector (3X) could not be assessed.

Localization of PRAF1 mutants in CHO cells and Golgi morphology were different between CHO and AtT-20 cells when PRAF(Y73A) and PRAF(N70T) were stably transfected. CHO cells stably transfected with a vector containing PRAF(N70T) are characterized by retention of PRAF1 in the endoplasmic reticulum (ER) while in those stably transfected with a PRAF(Y73A) vector, PRAF1 localizes to the ER, Golgi complex, and dense tubular structures.[19] Further, in CHO cells stably transfected with PRAF(N70T) and PRAF(H166A), a mutation expected to have effects similar to PRAF(Y73A), mannosidase II (Man II), a resident Golgi protein, is dispersed around the

nucleus and in punctate regions throughout the cytoplasm.[19] The difference between the appearance in AtT-20 cells and CHO cells may be due to the method of Golgi complex localization, i.e. staining for Man II vs. giantin as in our study. Since Man II transits through the Golgi complex and is then recycled from the trans to the cis face, dispersed localization of Man II throughout the stably transfected CHO cells suggests that Man II recycling was impaired.[19] In comparison, giantin acts as a tethering protein which cross-links the Golgi stacks and is not recycled through the Golgi complex.[208] Second, the differences seen in PRAF1 distribution between AtT-20 and CHO cells may be due to differences in the functions of PRAF1 in these cells. Lastly, it is possible that the tag used on the PRAF1 construct – hemagglutinin in CHO cells vs. FLAG in our study – may have influenced localization.

In cells stably transfected with full length (FL) PRAF1, PRAF1 and ACTH-containing peptide were evenly co-distributed and co-localized in the Golgi complex and ACTH-containing peptide was distributed along the plasma membrane in a pattern comparable to that of WT and 3X. PRAF1 was also identified in a few punctate regions in the cytoplasm in a pattern like that observed in CHO cells.[19] In accordance with subcellular fractionation studies, punctate staining suggests association of PRAF1 with intracellular vesicular membranes.[144]

Our results regarding basal ACTH secretion and ACTH and PRAF1 localization may indicate that a PRAF1/Rab3A interaction is necessary in AtT-20 cells for transit of POMC/ACTH-containing secretory vesicles from the Golgi complex to the plasma membrane via the regulated pathway. In murine synaptosomes, secretory vesicles travel from the Golgi complex to the plasma membrane via the regulated pathway and Rab3A

is essential for this activity.[90,209,210] Secretory vesicles enter the constitutive pathway by default if not associated with Rab3A.[71,80,141,211] If the same occurs in AtT-20 cells and not just Rab3A but a PRAF1/Rab3A interaction is required for movement of secretory vesicles, basal secretion of ACTH would be expected to be higher when the interaction does not occur. PRAF(54-175) and PRAF(54-112) likely do not interact with Rab3A, since the sites necessary for interaction[18] have been deleted, and, indeed, basal ACTH secretion was significantly higher in cells stably transfected with these constructs than in WT cells. Further, these stably transfected cells had reduced co-localization of ACTH and PRAF1 proteins in the Golgi complex compared to FL stable transfectants. PRAF1 is distributed in the cytoplasm in a punctate staining pattern in cell stably transfected with PRAF(54-175) and PRAF(54-112) suggesting PRAF1 protein is associated with intracellular vesicles. However, disrupted association of PRAF1 and ACTH-containing peptide may suggest that PRAF1 is not incorporated into ACTH-containing secretory vesicles and, as a result, Rab3A may not associate with secretory vesicle either.

Since secretion differed between the cell lines, we theorized that POMC processing might be affected. Therefore, we assayed the effect of the PRAF1 mutations on POMC processing by Western blotting of stably transfected AtT-20 cell lysates. We first performed Western blotting to ensure that all cell lines were expressing equivalent amounts of PRAF1 protein, so that differences between cell lines could not be attributed to variation in PRAF1. FL, PRAF(N70T), PRAF(Y73A), and PRAF(V161A) proteins were detected as doublets on the Western blot of the lysates, while PRAF(54-175) and PRAF(54-112) were single bands. PRAF1 is predicted by sequence homology to undergo post-translational modification (i.e. glycosylation or alkylation) in the region of

amino acids 175-185.[212] As PRAF(54-175) and PRAF(54-112) proteins do not include the proposed sites for post-translational modification, only a single unmodified protein band was seen whereas, the doublets may reflect the presence of both modified and unmodified protein. Regardless, the amount of PRAF1 protein was not different between cell lines.

With respect to ACTH-containing peptide, in vehicle-treated cells, the ACTH/pre-ACTH and ACTH/POMC ratios and the amount of ACTH in FL, PRAF(54-175), PRAF(54-112), and PRAF(Y73A) stable transfectants were significantly decreased compared to WT (Table 1). The diminished ratio can be explained by a suppression of POMC processing leading to increased amounts of POMC and pre-ACTH and decreased mature ACTH concentration. A decrease in ACTH concentration could be due to misrouting of secretory granules into either the constitutive pathway, where storage does not occur, or into the degradation pathway. If POMC were misrouted into the degradation pathway, elevated basal secretion would not be expected as occurs in these 3 cell types. Thus, our findings suggest that in our stable transfectants, POMC is directed into the constitutive pathway.

In order for POMC processing to occur in secretory granules, POMC must be packaged into granules that exit the Golgi complex and travel via the regulated pathway to the plasma membrane. Rab3A is an important component of regulatory pathway-targeted secretory vesicles as vesicles not associated with Rab3A enter the constitutive secretory pathway.[71,80,141,211] PRAF1 may function as a Golgi complex GTPase sorting protein responsible for the inclusion of Rab GTPases into secretory vesicles.[157] Thus, if PRAF1 and Rab3A do not interact, Rab3A might not associate with secretory vesicles

and misdirection of ACTH into the constitutive pathway could occur. Indeed, CHO cells transfected with PRAF1 mutants that do not interact with Rab3A have inhibited Golgi to plasma membrane transport of secretory proteins.[19] When POMC travels to the plasma membrane via the constitutive pathway, cleavage into ACTH does not occur as successfully, resulting in unprocessed POMC and, thus, decreased amounts of mature ACTH arriving at the plasma membrane.[71,80,211] Additionally, granules in the constitutive pathway are not stored, providing another mechanism for decreased intracellular ACTH concentrations.

Packaging of POMC into secretory granules also requires interaction with carboxypeptidase E (CPE).[61,63,64,213] Membrane-bound CPE has several functions vital to POMC processing. CPE is the Golgi complex receptor for nascent POMC and translocates POMC into the Golgi complex.[213] CPE also guides POMC through the Golgi complex and aids in the incorporation of POMC into secretory granules destined for the regulated pathway.[61,63,64,213] To our knowledge a PRAF1/CPE interaction has not been investigated; however, if one exists and if the mutations in PRAF1 are disruptive to that interaction, then intra-Golgi transport of POMC and packaging of POMC into secretory granules of the regulated pathway could be inhibited by stable transfection with mutant PRAF1.

The mutant PRAF(V161A) protein interacted strongly with Rab3A, but cells stably transfected with this mutant still had decreased ACTH/POMC and ACTH/pre-ACTH ratios and lower ACTH concentrations. In this cell line, the decreased ratios and concentration might result from disrupted Rab recycling. GTP-bound Rabs are associated with membranes, and after GTP hydrolysis, GDI associates with and removes

GDP-bound Rabs from the membrane.[141,206,207] As GDI and PRAF1 have opposite and antagonistic roles with regard to Rab recycling,[162] the enhanced PRAF(V161A)/Rab3A interaction could be strong enough to prevent GDI-mediated removal of Rab3A-GDP from the Golgi membrane. As a result, in cells stably transfected with PRAF(V161A), Rab3A recycling and, therefore, vesicle trafficking would be inhibited, and POMC processing would be diminished. Indeed, in AtT-20 cells transfected with GTPase-deficient o-rab3 mutants, secretory vesicles do not transit to the plasma membrane.[144]

Interestingly, pre-ACTH was secreted into the media of all AtT-20 cells stably transfected with a PRAF-containing vector. Likely, this is a reflection of the altered POMC processing in the cells and increased intracellular concentrations of pre-ACTH. Since the 3X stable transfectants did not secrete pre-ACTH, transfection alone does not account for this activity.

The expression of POMC was at least 3 fold higher in cells stably transfected with a PRAF1 construct compared to WT and 3X stable transfectants. However, the degree of increase varied between cell types. PRAF1 overexpression in human embryonic kidney cells inhibits gene transcription via the T cell factor (TCF) transcription activator by binding to the TCF-signaling protein β-catenin.[214] Thus, if PRAF1 interacts with POMC transcription factors in AtT-20 cells, overexpression may have an inhibitory effect on factors that block POMC expression or a stimulatory effect on factors that increase POMC expression.

As determined by Western blot, the increase in POMC expression was not reflected by an increase in the cellular concentration of ACTH-containing peptide. One possible explanation is that POMC mRNA is degraded before or during translation.

Through as yet undiscovered mechanisms, cells can sense the presence of excess message and, in response, target nascent polypeptides associated with actively translating polyribosomes via RNA silencing mechanisms such as microRNA (miRNA) and small interfering RNA (siRNA).[215-218] Binding of siRNA or miRNA to messenger RNA forms a duplex that is either unable to be translated (miRNA/mRNA duplexes), or is cleaved by endonucleases, thus the POMC mRNA is not fully translated. Alternately, POMC mRNA may be translated, but export of nascent POMC protein from the endoplasmic reticulum (ER) is interrupted and, as a result, the nascent polypeptide is degraded. In yeast, Yip3, the homologue of PRAF1, interacts with the Rab homologue Yip1p.[219,220] Yip1p is required for both coatomer protein II (COP II) vesicle biogenesis and, along with Ypt1p, for packaging of proteins into COP II vesicles at the ER.[221] In both yeast and mammals, COP II vesicles are responsible for transporting nascent polypeptides from the ER to the Golgi complex, and disruption of this process due to inefficient ER export results in rapid degradation of the nascent polypeptides.[222-226] If PRAF1 acts similarly in AtT-20 cells, PRAF1 mutations could decrease the concentration of nascent POMC protein that arrives at the Golgi complex. As POMC expression is not affected in the intermediate time frame of glucocorticoid-mediated inhibition of stimulated ACTH secretion,[227,228] the elevated POMC transcription may be an artifact of PRAF1 overexpression and, therefore, may not be relevant.

Therefore, overall, our results may indicate that a PRAF1/Rab3A interaction may be essential for secretory vesicle trafficking from the Golgi to the plasma membrane via the regulated pathway. However, a PRAF1/VAMP2 interaction is likely not needed. Further, a moderate level of PRAF1/Rab3A interaction may be necessary for normal

intra-Golgi transport as a strong interaction was associated with inhibited intra-Golgi transport.

The results of this study further support the theory that Rab3A is involved in vesicular transport from the Golgi complex to the plasma membrane and that Rab3A may function as an inhibitor of vesicle fusion. In addition, a PRAF1/VAMP2 interaction may be vital for CRH-stimulated ACTH secretion, but a PRAF1/Rab3A interaction is not. Finally, Dexras1 may inhibit PRAF1/Rab3A/VAMP2 interaction, however, a functional interaction between PRAF1/Rab3A/VAMP2 may be necessary for Dex-induced inhibition of stimulated ACTH secretion in the intermediate time frame. Still, other factors may be involved since a moderate level of interaction between PRAF1 and Dexras1, Rab3A, and VAMP2 results in WT-like functioning as in FL, whereas enhanced interaction results in a paradoxical response to Dex treatment as in PRAF(V161A). Our findings further suggest that a functional PRAF1/Rab3A interaction may be vital for POMC processing, as intracellular ACTH concentration was diminished in stable transfectants where the PRAF1 mutation abolished PRAF1/Rab3A interaction.

The results of this research indicate that a PRAF1/Rab3A/VAMP2 interaction may be vital for stimulated secretion of ACTH. In addition, a possible mechanism for the role of Dexras1/PRAF1 interaction in the intermediate time frame of inhibition can be proposed. Rab3A is believed to inhibit premature VAMP2 activation, potentially by binding to PRAF1, thus blocking VAMP2 access.[18] In rat hippocampal neurons and bovine chromaffin cells, Rab3A-GTP is hydrolysed to Rab-GDP upon calcium influx.[99,200] If the same occurs in AtT-20 cells, Rab3A would be hydrolyzed upon CRH-

induced Ca^{2+} influx. GDI removal of Rab3A would result in PRAF1/VAMP2 interaction and subsequent VAMP2 activation. In the presence of Dexras1, the rate of CRH-stimulated secretion is reduced. Conceivably, when Rab3A is removed by GDI, Dexras1 can bind PRAF1 and block VAMP2 access. If the PRAF1/Dexras1 interaction is transient or temporary, Dexras1 can be displaced. When Dexras1 is displaced, VAMP2 may then be able to interact with PRAF1 and become activated. Therefore, in the presence of CRH even when Dexras1 is present, VAMP2 is still able to be activated, although not at the same rate as CRH stimulation alone. Alternately, Dexras1 may strongly bind to PRAF1 and be hard to displace, but the Dexras1 concentration may be low enough that it does not block all the sites of PRAF1/Rab3A/VAMP2 interaction and, therefore, some sites of interaction are still able to function and result in docking, fusion, and secretion.

	Yeast two-hybrid			ACTH secretion		Ratio in lysate vs. WT		
	Dexras1	Rab3A	VAMP2	CRH vs. Veh	Dex vs. CRH	ACTH/ POMC	ACTH/ pre-ACTH	Pre-ACTH/ POMC
FL	++	++	++	↑	↓	↓	↓	NSD
PRAF (54-175)	++	—*	—*	No	N/A	↓	↓	NSD
PRAF (54-112)	—	—*	—*	No	N/A	↓	↓	NSD
PRAF (N70T)	+++	—	—	No	N/A	NSD	NSD	NSD
PRAF (Y73A)	+++	—	+	↑↑	NE	↓	↓	NSD
PRAF (V161A)	+++	+++	+++	↑	↑	NSD	NSD	NSD

Table 1. Summary of results from the yeast two-hybrid assay, the cell function assay (ACTH secretion), and the ratios derived from the Western blots of the vehicle treated lysates. + = presence of an interaction (strength of interaction estimated by number of +); - = no interaction. * = assumed lack of interaction based on the deletions present and published data.[18] In the ACTH secretion columns, ↓ = ACTH secretion significantly decreased; ↑ = ACTH secretion significantly increased; No = no significant change in secretion; N/A = not assessable due to a lack of CRH response; NE = no effect, i.e. Dex was unable to inhibit CRH-stimulated secretion. In the ratio columns, ↓ = ratio significantly decreased compared to wild type (WT) vehicle-treated cells; NSD = no significant difference.

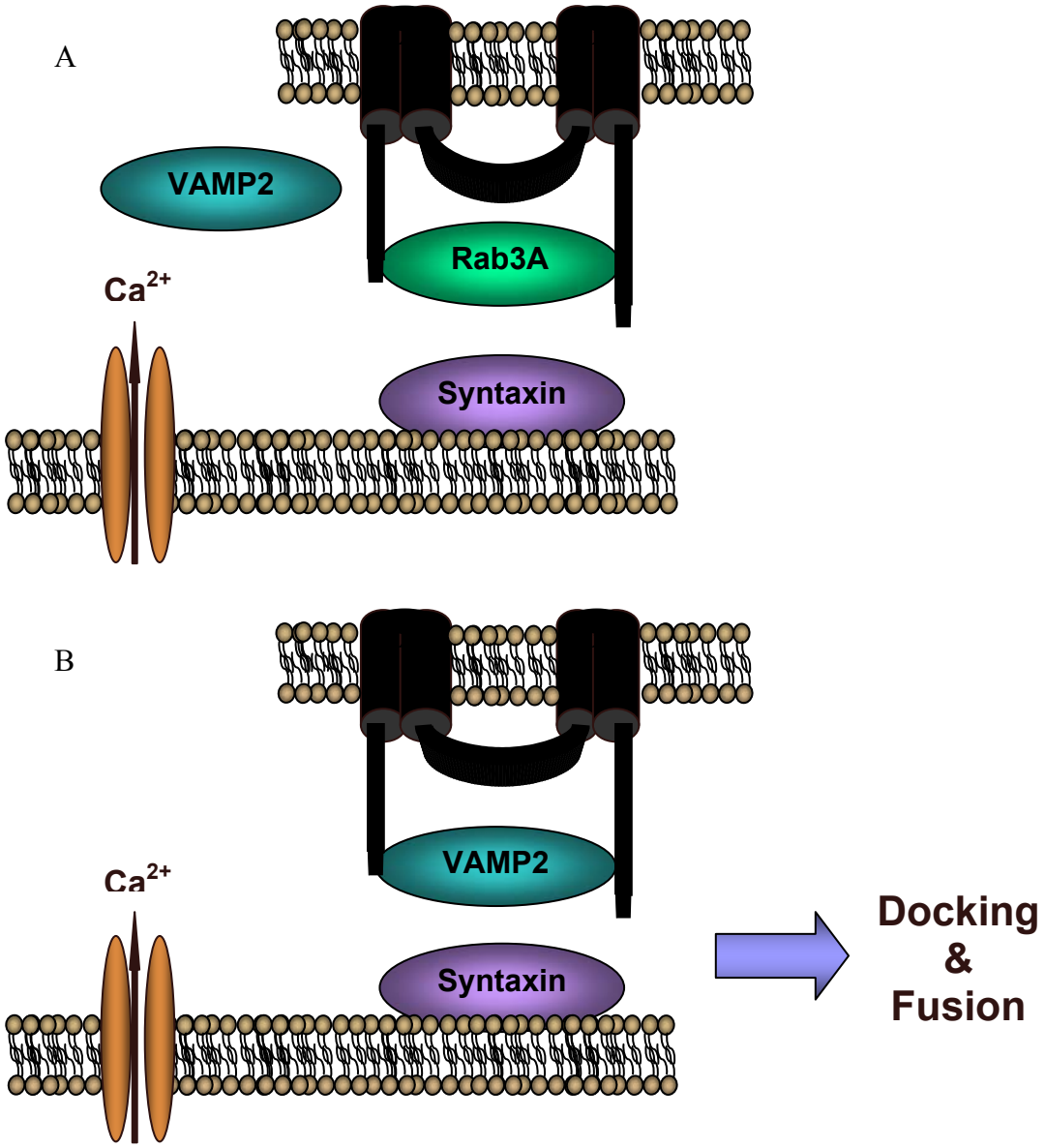

Figure 1. Proposed mechanism for the role of PRAF1 (black), Rab3A, and VAMP2 in stimulated ACTH secretion. A) Rab3A-GTP is bound to PRAF1 and blocks VAMP2 access. CRH-stimulated Ca2+ influx via voltage gated channels (brown ovals) induces GTP hydrolysis and Rab-GDP is removed. B) Removal of Rab3A allows VAMP2 access to PRAF1 and activation of VAMP2. VAMP2 interacts with syntaxin and docking and fusion follows.[18]

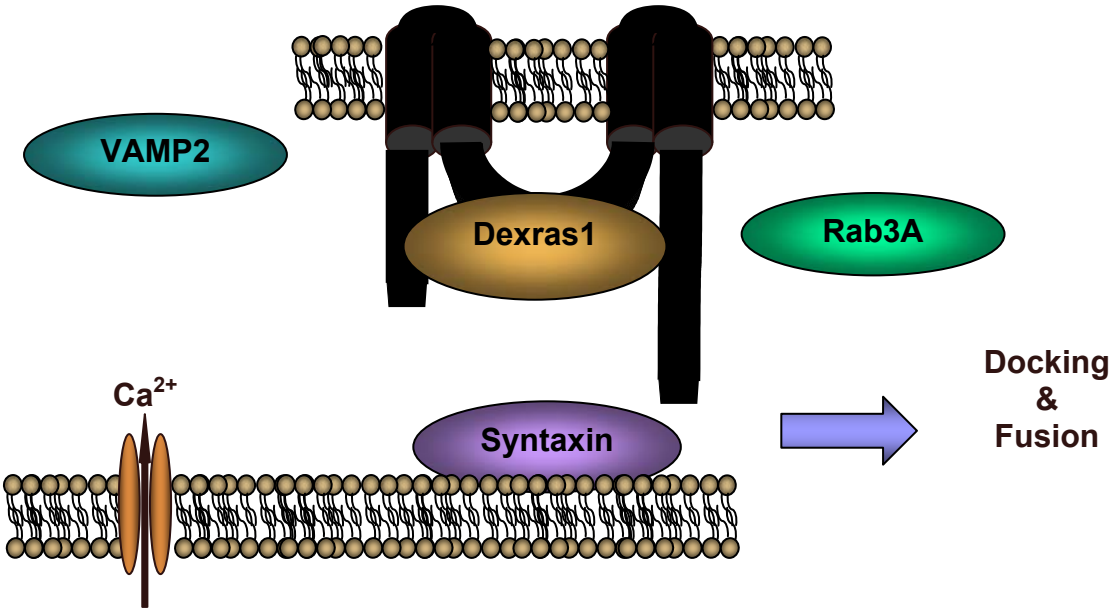

Figure 2. Proposed mechanism for the role of Dexras1 in Dex-mediated inhibition of stimulated ACTH secretion in the intermediate time frame. Dexras1 may inhibit both VAMP2 and Rab3A access to PRAF1 (black) by blocking the Rab3A/VAMP2 binding sites on PRAF1. As ACTH secretion still occurs, Dexras1 interaction with PRAF1 is either transient, or the concentration of Dexras1 may not be high enough to block all sites of membrane fusion.

Reference List

1. Compton, S. L. Characterization of the interaction between Dexras1 and PRA1. 1-59. 2004. Auburn University.Thesis

2. Antoni, F. A. Hypothalamic control of adrenocorticotropin secretion: advances since the discovery of 41-residue corticotropin-releasing factor. *Endocrinol Rev* **7**, 351-378 (1986).

3. Vale, W., Spiess, J., Rivier, C. & Rivier, J. Characterization of a 41-residue ovine hypothalamic peptide that stimulates secretion of corticotropin and beta-endorphin. *Science* **213**, 1394-1397 (1981).

4. Smets, G., Vauquelin, G., Moons, L., Smitz, J. & Kloppel, G. Receptors for corticotropin-releasing hormone in human pituitary: binding characteristics and autoradiographic localization to immunocytochemically defined proopiomelanocortin cells. *J Clin Endocrinol Metab* **73**, 268-274 (1991).

5. Childs, G. V., Morell, J. L., Niendorf, A. & Aguilera, G. Cytochemical studies of corticotropin-releasing factor (CRF) receptors in anterior lobe corticotropes: binding, glucocorticoid regulation, and endocytosis of [biotinyl-Ser1]CRF. *Endocrinology* **119**, 2129-2142 (1986).

6. Keller-Wood, M. E. & Dallman, M. F. Corticosteroid inhibition of ACTH secretion. *Endocrinol Rev* **5**, 1-24 (1984).

7. Antoni, F. A. & Dayanithi, G. Secretion of ACTH by perifused isolated rat anterior pituitary cells: pulses of secretagogue enhance the secretory response and modify the effect of atriopeptin. *J Endocrinol* **125**, 365-373 (1990).

8. Dayanithi, G. & Antoni, F. A. Rapid as well as delayed inhibitory effects of glucocorticoid hormones on pituitary adrenocorticotropic hormone release are mediated by type II glucocorticoid receptors and require newly synthesized messenger ribonucleic acid as well as protein. *Endocrinol* **125**, 308-313 (1989).

9. Tsigos, C. & Chrousos, G. P. Physiology of the hypothalamic-pituitary-adrenal axis in health and dysregulation in psychiatric and autoimmune disorders. *Endocrinol Metab Clin North Am.* **23**, 451-466 (1994).

10. Medvei, V. C. The history of Cushing's disease: a controversial tale. *J R Soc Med* **84**, 363-366 (1991).

11. Martin, A. & Reichlin, M. Corticotropin-releasing hormone in the hypercortisolism of depression and Cushing's disease. *New Eng J Med*. 316, 217-219. 1987. Abstract

12. Ludecke, D., Kautzky, R., Saeger, W. & Schrader, D. Selective removal of hypersecreting pituitary adenomas? An analysis of endocrine function, operative and microscopical findings in 101 cases. *Acta Neurochir. (Wien.)* **35**, 27-42 (1976).

13. Lamberts, S. W. *et al.* Failure of clinical remission after transsphenoidal removal of a microadenoma in a patient with Cushing's disease: multiple hyperplastic and adenomatous cell nets in surrounding pituitary tissue. *J Clin Endocrinol Metab* **50**, 793-795 (1980).

14. Cook, D. M. & McCarthy, P. J. Failure of hypophysectomy to correct pituitary-dependent Cushing's disease in two patients. *Arch Intern Med* **148**, 2497-2500 (1988).

15. Kemppainen, R. J. & Behrend, E. N. Dexamethasone rapidly induces a novel ras superfamily member-related gene in AtT-20 cells. *J Biol Chem* **273**, 3129-3131 (1998).

16. Graham, T. E., Key, T. A., Kilpatrick, K. & Dorin, R. I. Dexras1/AGS-1, a steroid hormone-induced guanosine triphosphate-binding protein, inhibits 3',5'-cyclic adenosine monophosphate-stimulated secretion in AtT-20 corticotroph cells. *Endocrinology* **142**, 2631-2640 (2001).

17. Behrend, E. N., Graham, T. E., Dorin, R. I. & Kemppainen, R. J. "Prenylated Rab Acceptor 1" interacts with Dexras1. *Proc 83rd Ann Meeting Endo Soc* 491. 2001. Abstract

18. Martincic, I., Peralta, M. E. & Ngsee, J. K. Isolation and characterization of a dual prenylated Rab and VAMP2 receptor. *J Biol Chem* **272**, 26991-26998 (1997).

19. Gougeon, P. Y., Prosser, D. C., Da-Silva, L. F. & Ngsee, J. K. Disruption of Golgi morphology and trafficking in cells expressing mutant prenylated rab acceptor-1. *J Biol Chem* **277**, 36408-36414 (2002).

20. *Canine and Feline Endocrinology and Repreduction*. Feldman, E. C. & Nelson, R. W. (eds.), pp. 137-194 (W.B. Saunders Company, Philidelphia,2004).

21. Orth, D. N. & Kovacs, W. J. *William's Textbook of Endocrinology*. W.B. Saunders Co., Philidelphia (1998).

22. Orth, D. N. Cushing's syndrome. *New Eng Med J* **332**, 791-803 (1995).

23. Gotch, P. M. Cushing's syndrome from the patient's perspective. *Endocrinol Metab Clin N Amer* **23**, 607-617 (1994).

24. Pelkonen, R. *et al.* Pituitary function after pituitary apoplexy. *Am J Med* **65**, 773-778 (1978).

25. Post, K. D. & Habas, J. E. Comparison of long term results between prolactin secreting adenomas and ACTH secreting adenomas. *Can J Neurol Sci* **17**, 74-77 (1990).

26. Robert, F. & Hardy, J. Cushing's disease: a correlation of radiological, surgical and pathological findings with therapeutic results. *Pathol Res Pract.* **187**, 617-621 (1991).

27. Bayever, E. & Iversen, P. Oligonucleotides in the treatment of leukemia. *Hematol Oncol* **12**, 9-14 (1994).

28. Jansen, B. *et al.* bcl-2 antisense therapy chemosensitizes human melanoma in SCID mice. *Nat Med* **4**, 232-234 (1998).

29. Bold, R. J., Alpard, S., Ishizuka, J., Townsend, C. M., Jr. & Thompson, J. C. Growth-regulatory effect of gastrin on human colon cancer cell lines is determined by protein kinase a isoform content. *Regul Pept* **53**, 61-70 (1994).

30. Nesterova, M. & Cho-Chung, Y. S. A single-injection protein kinase A-directed antisense treatment to inhibit tumour growth. *Nat Med* **1**, 528-533 (1995).

31. Murayama, Y. & Horiuchi, S. Antisense oligonucleotides to p53 tumor suppressor suppress the induction of apoptosis by epidermal growth factor in NCI-H 596 human lung cancer cells. *Antisense Nucleic Acid Drug Dev.* **7**, 109-114 (1997).

32. Casalini, P. *et al.* Inhibition of tumorigenicity in lung adenocarcinoma cells by c-erbB-2 antisense expression. *Int J Cancer* **72**, 631-636 (1997).

33. Akino, K. *et al.* Antisense inhibition of parathyroid hormone-related peptide gene expression reduces malignant pituitary tumor progression and metastases in the rat. *Cancer Res* **56**, 77-86 (1996).

34. Missale, C. *et al.* Nerve growth factor controls proliferation and progression of human prolactinoma cell lines through an autocrine mechanism. *Mol Endocrinol* **10**, 272-285 (1996).

35. Woloschak, M., Post, K. & Roberts, J. L. Effects of antisense DNA on POMC mRNA and ACTH levels in cultured human corticotroph adenoma cells. *J Endocrinol Invest* **17**, 817-819 (1994).

36. Frankel, B., Longo, S. L., Rodziewicz, G. S. & Hodge, C. J., Jr. Antisense oligonucleotide-induced inhibition of adrenocorticotropic hormone release from cultured human corticotrophs. *J Neurosurg.* **91**, 261-267 (1999).

37. Phillips, M. & Tashjian, A. H., Jr. Characterization of an early inhibitory effect of glucocorticoids on stimulated adrenocorticotropin and endorphin release from a clonal strain of mouse pituitary cells. *Endocrinology* **110**, 892-900 (1982).

38. Shipston, M. J. & Antoni, F. A. Early glucocorticoid feedback in anterior pituitary corticotrophs: differential inhibition of hormone release induced by vasopressin and corticotrophin-releasing factor in vitro. *J Endocrinol* **129**, 261-268 (1991).

39. Yalow, R. S. & Berson, S. A. Size heterogeneity of immunoreactive human ACTH in plasma and in extracts of pituitary glands and ACTH-producing thymoma. *Biochem Biophys Res Commun* **44**, 439-445 (1971).

40. Bertagna, X. Y. *et al.* Corticotropin, lipotropin, and beta-endorphin production by a human nonpituitary tumor in culture: evidence for a common precursor. *Proc Natl Acad Sci U. S. A* **75**, 5160-5164 (1978).

41. Mains, R. E., Eipper, B. A. & Ling, N. Common precursor to corticotropins and endorphins. *Proc Natl Acad Sci U. S. A* **74**, 3014-3018 (1977).

42. Chang, A. C., Cochet, M. & Cohen, S. N. Structural organization of human genomic DNA encoding the pro-opiomelanocortin peptide. *Proc Natl Acad Sci U. S. A* **77**, 4890-4894 (1980).

43. Drouin, J. & Goodman, H. M. Most of the coding region of rat ACTH beta--LPH precursor gene lacks intervening sequences. *Nature* **288**, 610-613 (1980).

44. Boileau, G., Barbeau, C., Jeannotte, L., Chretien, M. & Drouin, J. Complete structure of the porcine pro-opiomelanocortin mRNA derived from the nucleotide sequence of cloned cDNA. *Nucleic Acids Res* **11**, 8063-8071 (1983).

45. Lundblad, J. R. & Roberts, J. L. Regulation of proopiomelanocortin gene expression in pituitary. *Endocrinol Rev* **9**, 135-158 (1988).

46. Labrie, F. *et al.* Corticotropin-releasing factor stimulates accumulation of adenosine 3', 5'-monophosphate in rat pituitary corticotrophs. *Science* **216**, 1007-1008 (1982).

47. Aguilera, G. *et al.* Mechanisms of action of corticotropin-releasing factor and other regulators of corticotropin release in rat pituitary cells. *J Biol Chem* **258**, 8039-8045 (1983).

48. Clark, T. P. & Kemppainen, R. J. Glucocorticoids do not affect intracellular calcium transients in corticotrophs: evidence supporting an effect distal to calcium influx. *Neuroendocrinol* **60**, 273-282 (1994).

49. Guild, S. & Reisine, T. Molecular mechanisms of corticotropin-releasing factor stimulation of calcium mobilization and adrenocorticotropin release from anterior pituitary tumor cells. *J Pharmacol Exp Ther.* **241**, 125-130 (1987).

50. Reisine, T., Rougon, G., Barbet, J. & Affolter, H. U. Corticotropin-releasing factor-induced adrenocorticotropin hormone release and synthesis is blocked by incorporation of the inhibitor of cyclic AMP-dependent protein kinase into anterior pituitary tumor cells by liposomes. *Proc Natl Acad Sci U. S. A* **82**, 8261-8265 (1985).

51. Rougon, G., Barbet, J. & Reisine, T. Protein phosphorylation induced by phorbol esters and cyclic AMP in anterior pituitary cells: possible role in adrenocorticotropin release and synthesis. *J Neurochem* **52**, 1270-1278 (1989).

52. Vyas, S., Bishop, J. F., Gehlert, D. R. & Patel, J. Effects of protein kinase C down-regulation on secretory events and proopiomelanocortin gene expression in anterior pituitary tumor (AtT-20) cells. *J Neurochem* **54**, 248-255 (1990).

53. Civelli, O., Birnberg, N. & Herbert, E. Detection and quantitation of pro-opiomelanocortin mRNA in pituitary and brain tissues from different species. *J Biol Chem* **257**, 6783-6787 (1982).

54. Gee, C. E., Chen, C. L., Roberts, J. L., Thompson, R. & Watson, S. J. Identification of proopiomelanocortin neurones in rat hypothalamus by in situ cDNA-mRNA hybridization. *Nature* **306**, 374-376 (1983).

55. Jeannotte, L., Burbach, J. P. & Drouin, J. Unusual proopiomelanocortin ribonucleic acids in extrapituitary tissues: intronless transcripts in testes and long poly(A) tails in hypothalamus. *Mol Endocrinol* **1**, 749-757 (1987).

56. Raffin-Sanson, M. L. *et al.* High precursor level in maternal blood results from the alternate mode of proopiomelanocortin processing in human placenta. *Clin Endocrinol (Oxf)* **50**, 85-94 (1999).

57. Raffin-Sanson, M. L. *et al.* Pro-opiomelanocortin in human pregnancy: evolution of maternal plasma levels, concentrations in cord blood, amniotic fluid and at the feto-maternal interface. *Eur. J Endocrinol* **142**, 53-59 (2000).

58. Schauer, E. *et al.* Proopiomelanocortin-derived peptides are synthesized and released by human keratinocytes. *J Clin Invest* **93**, 2258-2262 (1994).

59. Scholzen, T. E. *et al.* Expression of proopiomelanocortin peptides in human dermal microvascular endothelial cells: evidence for a regulation by ultraviolet light and interleukin-1. *J Invest Dermatol* **115**, 1021-1028 (2000).

60. Wintzen, M., Yaar, M., Burbach, J. P. & Gilchrest, B. A. Proopiomelanocortin gene product regulation in keratinocytes. *J Invest Dermatol* **106**, 673-678 (1996).

61. Cool, D. R., Fenger, M., Snell, C. R. & Loh, Y. P. Identification of the sorting signal motif within pro-opiomelanocortin for the regulated secretory pathway. *J Biol Chem* **270**, 8723-8729 (1995).

62. Tam, W. W., Andreasson, K. I. & Loh, Y. P. The amino-terminal sequence of pro-opiomelanocortin directs intracellular targeting to the regulated secretory pathway. *Eur J Cell Biol* **62**, 294-306 (1993).

63. Cool, D. R. *et al.* Carboxypeptidase E is a regulated secretory pathway sorting receptor: genetic obliteration leads to endocrine disorders in Cpe(fat) mice. *Cell* **88**, 73-83 (1997).

64. Shen, F. S. & Loh, Y. P. Intracellular misrouting and abnormal secretion of adrenocorticotropin and growth hormone in cpefat mice associated with a carboxypeptidase E mutation. *Proc Natl Acad Sci U. S. A* **94**, 5314-5319 (1997).

65. Roberts, J. L., Phillips, M., Rosa, P. A. & Herbert, E. Steps involved in the processing of common precursor forms of adrenocorticotropin and endorphin in cultures of mouse pituitary cells. *Biochemistry* **17**, 3609-3618 (1978).

66. Roberts, J. L., Phillips, M., Rosa, P. A., Budarf, M. & Herbert, E. Processing of common precursor forms of adrenocorticotropin and endorphins in cultures of mouse pituitary cells and in mouse pituitary. *Prog Clin Biol Res* **31**, 761-777 (1979).

67. Hook, V. Y. Differential distribution of carboxypeptidase-processing enzyme activity and immunoreactivity in membrane and soluble components of chromaffin granules. *J Neurochem* **45**, 987-989 (1985).

68. Fricker, L. D. & Devi, L. Posttranslational processing of carboxypeptidase E, a neuropeptide-processing enzyme, in AtT-20 cells and bovine pituitary secretory granules. *J Neurochem* **61**, 1404-1415 (1993).

69. Tooze, J., Hollinshead, M., Frank, R. & Burke, B. An antibody specific for an endoproteolytic cleavage site provides evidence that pro-opiomelanocortin is packaged into secretory granules in AtT20 cells before its cleavage. *J Cell Biol* **105**, 155-162 (1987).

70. Schnabel, E., Mains, R. E. & Farquhar, M. G. Proteolytic processing of pro-ACTH/endorphin begins in the Golgi complex of pituitary corticotropes and AtT-20 cells. *Mol Endocrinol* **3**, 1223-1235 (1989).

71. Tanaka, S., Yora, T., Nakayama, K., Inoue, K. & Kurosumi, K. Proteolytic processing of pro-opiomelanocortin occurs in acidifying secretory granules of AtT-20 cells. *J Histochem Cytochem* **45**, 425-436 (1997).

72. Gumbiner, B. & Kelly, R. B. Secretory granules of an anterior pituitary cell line, AtT-20, contain only mature forms of corticotropin and beta-lipotropin. *Proc Natl Acad Sci U. S. A* **78**, 318-322 (1981).

73. Benjannet, S., Rondeau, N., Day, R., Chretien, M. & Seidah, N. G. PC1 and PC2 are proprotein convertases capable of cleaving proopiomelanocortin at distinct pairs of basic residues. *Proc Natl Acad Sci U. S. A* **88**, 3564-3568 (1991).

74. Korner, J., Chun, J., Harter, D. & Axel, R. Isolation and functional expression of a mammalian prohormone processing enzyme, murine prohormone convertase 1. *Proc Natl Acad Sci U. S. A* **88**, 6834-6838 (1991).

75. Nakayama, K., Hosaka, M., Hatsuzawa, K. & Murakami, K. Cloning and functional expression of a novel endoprotease involved in prohormone processing at dibasic sites. *J Biochem (Tokyo)* **109**, 803-806 (1991).

76. Thomas, L. *et al.* Kex2-like endoproteases PC2 and PC3 accurately cleave a model prohormone in mammalian cells: evidence for a common core of neuroendocrine processing enzymes. *Proc Natl Acad Sci U. S. A* **88**, 5297-5301 (1991).

77. Moriyama, Y. & Futai, M. Presence of 5-hydroxytryptamine (serotonin) transport coupled with vacuolar-type H(+)-ATPase in neurosecretory granules from bovine posterior pituitary. *J Biol Chem* **265**, 9165-9169 (1990).

78. Nelson, N. & Taiz, L. The evolution of H+-ATPases. *Trends Biochem Sci* **14**, 113-116 (1989).

79. Mains, R. E. & May, V. The role of a low pH intracellular compartment in the processing, storage, and secretion of ACTH and endorphin. *J Biol Chem* **263**, 7887-7894 (1988).

80. Tanaka, S., Nomizu, M. & Kurosumi, K. Intracellular sites of proteolytic processing of pro-opiomelanocortin in melanotrophs and corticotrophs in rat pituitary. *J Histochem Cytochem* **39**, 809-821 (1991).

81. Lamango, N. S., Zhu, X. & Lindberg, I. Purification and enzymatic characterization of recombinant prohormone convertase 2: stabilization of activity by 21 kDa 7B2. *Arch Biochem Biophys* **330**, 238-250 (1996).

82. Martinez, O. & Goud, B. Rab proteins. *Biochim Biophys Acta* **1404**, 101-112 (1998).

83. Jackson, M. R., Nilsson, T. & Peterson, P. A. Retrieval of transmembrane proteins to the endoplasmic reticulum. *J Cell Biol* **121**, 317-333 (1993).

84. Chen, Y. A. & Scheller, R. H. SNARE-mediated membrane fusion. *Nat Rev Mol Cell Biol* **2**, 98-106 (2001).

85. McBride, H. M. *et al.* Oligomeric complexes link Rab5 effectors with NSF and drive membrane fusion via interactions between EEA1 and syntaxin 13. *Cell* **98**, 377-386 (1999).

86. Nielsen, E. *et al.* Rabenosyn-5, a novel Rab5 effector, is complexed with hVPS45 and recruited to endosomes through a FYVE finger domain. *J Cell Biol* **151**, 601-612 (2000).

87. Peterson, M. R., Burd, C. G. & Emr, S. D. Vac1p coordinates Rab and phosphatidylinositol 3-kinase signaling in Vps45p-dependent vesicle docking/fusion at the endosome. *Curr Biol* **9**, 159-162 (1999).

88. Seals, D. F., Eitzen, G., Margolis, N., Wickner, W. T. & Price, A. A Ypt/Rab effector complex containing the Sec1 homolog Vps33p is required for homotypic vacuole fusion. *Proc Natl Acad Sci U. S. A* **97**, 9402-9407 (2000).

89. Tall, G. G., Hama, H., DeWald, D. B. & Horazdovsky, B. F. The phosphatidylinositol 3-phosphate binding protein Vac1p interacts with a Rab GTPase and a Sec1p homologue to facilitate vesicle-mediated vacuolar protein sorting. *Mol Biol Cell* **10**, 1873-1889 (1999).

90. Geppert, M. *et al.* The role of Rab3A in neurotransmitter release. *Nature* **369**, 493-497 (1994).

91. Vicogne, J. *et al.* Asymmetric phospholipid distribution drives in vitro reconstituted SNARE-dependent membrane fusion. *PNAS* **103**, 14761-14766 (2006).

92. Mollinedo, F., Martin-Martin, B., Calafat, J., Nabokina, S. M. & Lazo, P. A. Role of Vesicle-Associated Membrane Protein-2, Through Q-Soluble N-Ethylmaleimide-Sensitive Factor Attachment Protein Receptor/R-Soluble N-Ethylmaleimide-Sensitive Factor Attachment Protein Receptor Interaction, in the Exocytosis of Specific and Tertiary Granules of Human Neutrophils. *J Immunol* **170**, 1034-1042 (2003).

93. Logan, M. R., Lacy, P., Bablitz, B. & Moqbel, R. Expression of eosinophil target SNAREs as potential cognate receptors for vesicle-associated membrane protein-2 in exocytosis. *J Allergy Clin Immunol* **109**, 299-306 (2002).

94. Holz, R. W., Brondyk, W. H., Senter, R. A., Kuizon, L. & Macara, I. G. Evidence for the involvement of Rab3A in Ca(2+)-dependent exocytosis from adrenal chromaffin cells. *J Biol Chem* **269**, 10229-10234 (1994).

95. Johannes, L. *et al.* The GTPase Rab3a negatively controls calcium-dependent exocytosis in neuroendocrine cells. *EMBO J* **13**, 2029-2037 (1994).

96. Johannes, L. *et al.* Regulation of the Ca2+ sensitivity of exocytosis by Rab3a. *J Neurochem* **71**, 1127-1133 (1998).

97. Regazzi, R. *et al.* Expression, localization and functional role of small GTPases of the Rab3 family in insulin-secreting cells. *J Cell Sci* **109 (Pt 9)**, 2265-2273 (1996).

98. Fischer von, M. G., Stahl, B., Li, C., Sudhof, T. C. & Jahn, R. Rab proteins in regulated exocytosis. *Trends Biochem Sci* **19**, 164-168 (1994).

99. Star, E. N., Newton, A. J. & Murthy, V. N. Real-time imaging of Rab3a and Rab5a reveals differential roles in presynaptic function. *J Physiol* **569**, 103-117 (2005).

100. Alory, C. & Balch, W. E. Molecular evolution of the Rab-escort-protein/guanine-nucleotide-dissociation-inhibitor superfamily. *Mol Biol Cell* **14**, 3857-3867 (2003).

101. Autelitano, D. J., Lundblad, J. R., Blum, M. & Roberts, J. L. Hormonal regulation of POMC gene expression. *Annu Rev Physiol* **51**, 715-726 (1989).

102. Svec, F. Comparison of glucocorticoid receptor depletion and the suppression of ACTH secretion in the AtT-20 cell. *J Steroid Biochem* **20**, 821-827 (1984).

103. Clark, T. P. & Kemppainen, R. J. Glucocorticoid negative feedback in sheep corticotrophs: a comparison with AtT-20 corticotroph tumor cells. *Am J Physiol* **267**, R463-R469 (1994).

104. Woods, M. D., Shipston, M. J., Mullens, E. L. & Antoni, F. A. Pituitary corticotrope tumor (AtT20) cells as a model system for the study of early inhibition by glucocorticoids. *Endocrinology* **131**, 2873-2880 (1992).

105. Guerineau, N., Corcuff, J. B., Tabarin, A. & Mollard, P. Spontaneous and corticotropin-releasing factor-induced cytosolic calcium transients in corticotrophs. *Endocrinology* **129**, 409-420 (1991).

106. Won, J. G., Oki, Y. & Orth, D. N. Roles of intracellular and extracellular calcium in the kinetic profile of adrenocorticotropin secretion by perifused rat anterior pituitary cells. II. Arginine vasopressin, oxytocin, and angiotensin-II stimulation. *Endocrinology* **126**, 858-868 (1990).

107. Won, J. G. & Orth, D. N. Roles of intracellular and extracellular calcium in the kinetic profile of adrenocorticotropin secretion by perifused rat anterior pituitary cells. I. Corticotropin-releasing factor stimulation. *Endocrinology* **126**, 849-857 (1990).

108. Loechner, K. J., Kream, R. M. & Dunlap, K. Calcium currents in a pituitary cell line (AtT-20): differential roles in stimulus-secretion coupling. *Endocrinology* **137**, 1429-1437 (1996).

109. Woods, M. D., Shipston, M. J., McFerran, B., Guild, S. B. & Antoni, F. A. Early glucocorticoid inhibition of hormone release in pituitary corticotrope cells is voltage dependent. *Ann N. Y. Acad Sci* **746**, 456-459 (1994).

110. Antoni, F. A., Hoyland, J., Woods, M. D. & Mason, W. T. Glucocorticoid inhibition of stimulus-evoked adrenocorticotrophin release caused by suppression of intracellular calcium signals. *J Endocrinol* **133**, R13-R16 (1992).

111. Pennington, A. J., Kelly, J. S. & Antoni, F. A. Selective enhancement of an A type potassium current by dexamethasone in a corticotroph cell line. *J Neuroendocrinol* **6**, 305-315 (1994).

112. Shipston, M. J., Kelly, J. S. & Antoni, F. A. Glucocorticoids block protein kinase A inhibition of calcium-activated potassium channels. *J Biol Chem* **271**, 9197-9200 (1996).

113. Lim, M. C., Shipston, M. J. & Antoni, F. A. Depolarization counteracts glucocorticoid inhibition of adenohypophysical corticotroph cells. *Br J Pharmacol* **124**, 1735-1743 (1998).

114. Link, H., Dayanithi, G. & Gratzl, M. Glucocorticoids rapidly inhibit oxytocin-stimulated adrenocorticotropin release from rat anterior pituitary cells, without modifying intracellular calcium transients. *Endocrinology* **132**, 873-878 (1993).

115. Aunis, D., Hesketh, J. E. & Devilliers, G. Freeze-fracture study of the chromaffin cell during exocytosis: evidence for connections between the plasma membrane and secretory granules and for movements of plasma membrane-associated particles. *Cell Tissue Res* **197**, 433-441 (1979).

116. Aunis, D. & Perrin, D. Chromaffin granule membrane-F-actin interactions and spectrin-like protein of subcellular organelles: a possible relationship. *J Neurochem* **42**, 1558-1569 (1984).

117. Aunis, D. & Bader, M. F. The cytoskeleton as a barrier to exocytosis in secretory cells. *J Exp Biol* **139**, 253-266 (1988).

118. Burgess, L. E. *et al.* Potent selective nonpeptidic inhibitors of human lung tryptase. *Proc Natl Acad Sci U. S. A* **96**, 8348-8352 (1999).

119. Castellino, F., Heuser, J., Marchetti, S., Bruno, B. & Luini, A. Glucocorticoid stabilization of actin filaments: a possible mechanism for inhibition of corticotropin release. *Proc Natl Acad Sci USA* **89**, 3775-3779 (1992).

120. Arimura, A., Bowers, C. Y., Schally, A. V., Saito, M. & Miller, M. C., III Effect of corticotropin-releasing factor, dexamethasone and actinomycin D on the release of ACTH from rat pituitaries in vivo and in vitro. *Endocrinology* **85**, 300-311 (1969).

121. Cismowski, M. J. *et al.* Genetic screens in yeast to identify mammalian nonreceptor modulators of G-protein signaling. *Nat Biotechnol* **17**, 878-883 (1999).

122. Falk, J. D. *et al.* Rhes: A striatal-specific Ras homolog related to Dexras1. *J Neurosci Res* **57**, 782-788 (1999).

123. St Croix B. *et al.* Genes expressed in human tumor endothelium. *Science* **289**, 1197-1202 (2000).

124. Tu, Y. & Wu, C. Cloning, expression and characterization of a novel human Ras-related protein that is regulated by glucocorticoid hormone. *Biochimica et Biophysica Acta (BBA) - Gene Structure and Expression* **1489**, 452-456 (1999).

125. Bourne, H. R., Sanders, D. A. & McCormick, F. The GTPase superfamily: conserved structure and molecular mechanism. *Nature* **349**, 117-127 (1991).

126. Zerial, M. & Stenmark, H. Rab GTPases in vesicular transport. *Curr Opin Cell Biol* **5**, 613-620 (1993).

127. Kemppainen, R., Behrend, E. N., Brogan, M. D. & Ammons, J. M. Cloning and characterization of the human Dexras1 gene. *Proceedings of the 82nd Annual Meeting of the Endocrine Society* . 2000. Abstract

128. Kemppainen, R. J. & Behrend, E. N. Enhancement of secretagogue-induced adrenocorticotropic hormone release from cultured sheep anterior pituitary cells by recombinant ovine interleukin 1. *Am J Vet Res* **59**, 107-110 (1998).

129. Cismowski, M. J. *et al.* Activation of heterotrimeric G-protein signaling by a ras-related protein. Implications for signal integration. *J Biol Chem* **275**, 23421-23424 (2000).

130. Luini, A., Lewis, D., Guild, S., Schofield, G. & Weight, F. Somatostatin, an inhibitor of ACTH secretion, decreases cytosolic free calcium and voltage-dependent calcium current in a pituitary cell line. *J Neurosci* **6**, 3128-3132 (1986).

131. Reisine, T., Wang, H. L. & Guild, S. Somatostatin inhibits cAMP-dependent and cAMP-independent calcium influx in the clonal pituitary tumor cell line AtT-20 through the same receptor population. *J Pharmacol Exp Ther* **245**, 225-231 (1988).

132. Graham, T. E., Prossnitz, E. R. & Dorin, R. I. Dexras1/AGS-1 inhibits signal transduction from the Gi-coupled formyl peptide receptor to Erk-1/2 MAP kinases. *J Biol Chem* **277**, 10876-10882 (2002).

133. Takesono, A., Nowak, M. W., Cismowski, M., Duzic, E. & Lanier, S. M. Activator of G-protein signaling 1 blocks GIRK channel activation by a G-protein-coupled receptor: apparent disruption of receptor signaling complexes. *J Biol Chem* **277**, 13827-13830 (2002).

134. McCormick, F. Ras-related proteins in signal transduction and growth control. *Mol Reprod Dev* **42**, 500-506 (1995).

135. Martelli, A. M. *et al.* Diffuse vesicular distribution of Rab3D in the polarized neuroendocrine cell line AtT-20. *FEBS Lett* **368**, 271-275 (1995).

136. Birnberg, N. C., Stork, P. J. & Hemmick, L. M. Expression of the c-Harvey ras oncogene alters peptide synthesis in the neurosecretory cell line AtT20. *J Biol Chem* **267**, 15464-15468 (1992).

137. Chandler, L. A., Ehretsmann, C. P. & Bourgeois, S. A novel mechanism of Ha-ras oncogene action: regulation of fibronectin mRNA levels by a nuclear posttranscriptional event. *Mol Cell Biol* **14**, 3085-3093 (1994).

138. Riis, B., Rattan, S. I., Clark, B. F. & Merrick, W. C. Eukaryotic protein elongation factors. *Trends Biochem Sci* **15**, 420-424 (1990).

139. Johnson, D. I. Cdc42: An essential Rho-type GTPase controlling eukaryotic cell polarity. *Microbiol Mol Biol Rev* **63**, 54-105 (1999).

140. Kjoller, L. & Hall, A. Signaling to Rho GTPases. *Exp Cell Res* **253**, 166-179 (1999).

141. Novick, P. & Zerial, M. The diversity of Rab proteins in vesicle transport. *Curr Opin Cell Biol* **9**, 496-504 (1997).

142. Pfeffer, S. R. Rab GTPases: master regulators of membrane trafficking. *Curr Opin Cell Biol* **6**, 522-526 (1994).

143. Baldini, G. *et al.* Expression of Rab3D N135I inhibits regulated secretion of ACTH in AtT-20 cells. *J Cell Biol* **140**, 305-313 (1998).

144. Ngsee, J. K., Fleming, A. M. & Scheller, R. H. A rab protein regulates the localization of secretory granules in AtT-20 cells. *Mol Biol Cell* **4**, 747-756 (1993).

145. Bucci, C. *et al.* The small GTPase rab5 functions as a regulatory factor in the early endocytic pathway. *Cell* **70**, 715-728 (1992).

146. Fang, M. *et al.* Dexras1: a G protein specifically coupled to neuronal nitric oxide synthase via CAPON. *Neuron* **28**, 183-193 (2000).

147. Kemppainen, R. J., Clark, T. P., Sartin, J. L. & Zerbe, C. A. Hypothalamic peptide regulation of ACTH secretion from sheep pituitary. *Am J Physiol* **265**, R840-R845 (1993).

148. Hard, M. L., Abdolell, M., Robinson, B. H. & Koren, G. Gene-expression analysis after alcohol exposure in the developing mouse. *J Lab Clin Med* **145**, 47-54 (2005).

149. Kimura, K. A. & Brien, J. F. Hippocampal nitric oxide synthase in the fetal guinea pig: effects of chronic prenatal ethanol exposure. *Brain Res Dev Brain Res* **106**, 39-46 (1998).

150. Bonthius, D. J. *et al.* Deficiency of neuronal nitric oxide synthase (nNOS) worsens alcohol-induced microencephaly and neuronal loss in developing mice. *Brain Res Dev Brain Res* **138**, 45-59 (2002).

151. Kimura, K. A., Parr, A. M. & Brien, J. F. Effect of chronic maternal ethanol administration on nitric oxide synthase activity in the hippocampus of the mature fetal guinea pig. *Alcohol Clin Exp Res* **20**, 948-953 (1996).

152. Bucci, C., Chiariello, M., Lattero, D., Maiorano, M. & Bruni, C. B. Interaction cloning and characterization of the cDNA encoding the human prenylated rab acceptor (PRA1). *Biochem Biophys Res Commun* **258**, 657-662 (1999).

153. Liang, Z. & Li, G. Mouse prenylated Rab acceptor is a novel Golgi membrane protein. *Biochem Biophys Res Commun.* **275**, 509-516 (2000).

154. Fo, C. S., Coleman, C. S., Wallick, C. J., Vine, A. L. & Bachmann, A. S. Genomic organization, expression profile, and characterization of the new protein PRA1 domain family, member 2 (PRAF2). *Gene* **371**, 154-165 (2006).

155. Abdul-Ghani, M., Gougeon, P. Y., Prosser, D. C., Da-Silva, L. F. & Ngsee, J. K. PRA isoforms are targeted to distinct membrane compartments. *J Biol Chem* **276**, 6225-6233 (2001).

156. Fenster, S. D. *et al.* Piccolo, a presynaptic zinc finger protein structurally related to bassoon. *Neuron* **25**, 203-214 (2000).

157. Figueroa, C., Taylor, J. & Vojtek, A. B. Prenylated Rab acceptor protein is a receptor for prenylated small GTPases. *J Biol Chem* **276**, 28219-28225 (2001).

158. Sivars, U., Aivazian, D. & Pfeffer, S. Purification and properties of Yip3/PRA1 as a Rab GDI displacement factor. *Methods Enzymol* **403**, 348-356 (2005).

159. Nishimura, N. & Balch, W. E. A di-acidic signal required for selective export from the endoplasmic reticulum. *Science* **277**, 556-558 (1997).

160. Nishimura, N. *et al.* A di-acidic (DXE) code directs concentration of cargo during export from the endoplasmic reticulum. *J Biol Chem* **274**, 15937-15946 (1999).

161. Lin, J., Liang, Z., Zhang, Z. & Li, G. Membrane topography and topogenesis of prenylated Rab acceptor (PRA1). *J Biol Chem* **276**, 41733-41741 (2001).

162. Hutt, D. M., Da-Silva, L. F., Chang, L. H., Prosser, D. C. & Ngsee, J. K. PRA1 inhibits the extraction of membrane-bound rab GTPase by GDI1. *J Biol Chem* **275**, 18511-18519 (2000).

163. Liang, Z., Veeraprame, H., Bayan, N. & Li, G. The C-terminus of prenylin is important in forming a dimer conformation necessary for endoplasmic-reticulum-to-Golgi transport. *Biochem J* **380**, 43-49 (2004).

164. Daro, E., van der, S. P., Galli, T. & Mellman, I. Rab4 and cellubrevin define different early endosome populations on the pathway of transferrin receptor recycling. *Proc Natl Acad Sci U. S. A* **93**, 9559-9564 (1996).

165. Gorvel, J. P., Chavrier, P., Zerial, M. & Gruenberg, J. rab5 controls early endosome fusion in vitro. *Cell* **64**, 915-925 (1991).

166. Li, G., Barbieri, M. A., Colombo, M. I. & Stahl, P. D. Structural features of the GTP-binding defective Rab5 mutants required for their inhibitory activity on endocytosis. *J Biol Chem* **269**, 14631-14635 (1994).

167. McLauchlan, H. *et al.* A novel role for Rab5-GDI in ligand sequestration into clathrin-coated pits. *Curr Biol* **8**, 34-45 (1998).

168. Nielsen, E., Severin, F., Backer, J. M., Hyman, A. A. & Zerial, M. Rab5 regulates motility of early endosomes on microtubules. *Nat Cell Biol* **1**, 376-382 (1999).

169. Bucci, C., Thomsen, P., Nicoziani, P., McCarthy, J. & van, D. B. Rab7: a key to lysosome biogenesis. *Mol Biol Cell* **11**, 467-480 (2000).

170. Calero, M. & Collins, R. N. Saccharomyces cerevisiae Pra1p/Yip3p interacts with Yip1p and Rab proteins. *Biochem Biophys Res Commun* **290**, 676-681 (2002).

171. Li, L. Y., Shih, H. M., Liu, M. Y. & Chen, J. Y. The cellular protein PRA1 modulates the anti-apoptotic activity of Epstein-Barr virus BHRF1, a homologue of Bcl-2, through direct interaction. *J Biol Chem* **276**, 27354-27362 (2001).

172. Gross, A., McDonnell, J. M. & Korsmeyer, S. J. BCL-2 family members and the mitochondria in apoptosis. *Genes Dev* **13**, 1899-1911 (1999).

173. Foghsgaard, L. & Jaattela, M. The ability of BHRF1 to inhibit apoptosis is dependent on stimulus and cell type. *J Virol* **71**, 7509-7517 (1997).

174. Evans, D. T., Tillman, K. C. & Desrosiers, R. C. Envelope glycoprotein cytoplasmic domains from diverse lentiviruses interact with the prenylated Rab acceptor. *J Virol* **76**, 327-337 (2002).

175. Lodge, R., Lalonde, J. P., Lemay, G. & Cohen, E. A. The membrane-proximal intracytoplasmic tyrosine residue of HIV-1 envelope glycoprotein is critical for basolateral targeting of viral budding in MDCK cells. *EMBO J* **16**, 695-705 (1997).

176. Stephens, E. B. & Compans, R. W. Assembly of animal viruses at cellular membranes. *Annu Rev Microbiol* **42**, 489-516 (1988).

177. Strauss, J. H. & Strauss, E. G. Evolution of RNA viruses. *Annu Rev Microbiol* **42**, 657-683 (1988).

178. Varmus, H. Retroviruses. *Science* **240**, 1427-1435 (1988).

179. Morita, E. & Sundquist, W. I. Retrovirus budding. *Annu Rev Cell Dev Biol* **20**, 395-425 (2004).

180. Enouf, V., Chwetzoff, S., Trugnan, G. & Cohen, J. Interactions of rotavirus VP4 spike protein with the endosomal protein Rab5 and the prenylated Rab acceptor PRA1. *J Virol* **77**, 7041-7047 (2003).

181. Fiore, L., Greenberg, H. B. & Mackow, E. R. The VP8 fragment of VP4 is the rhesus rotaviral hemagglutinin. *Virology* **181**, 553-563 (1991).

182. Kirkwood, C. D., Bishop, R. F. & Coulson, B. S. Attachment and growth of human rotaviruses RV-3 and S12/85 in Caco-2 cells depend on VP4. *J Virol* **72**, 9348-9352 (1998).

183. Ludert, J. E. *et al.* Genetic mapping indicates that VP4 is the rotavirus cell attachment protein in vitro and in vivo. *J Virol* **70**, 487-493 (1996).

184. Crawford, S. E. *et al.* Trypsin cleavage stabilizes the rotavirus VP4 spike. *J Virol* **75**, 6052-6061 (2001).

185. Lopez, S., Arias, C. F., Bell, J. R., Strauss, J. H. & Espejo, R. T. Primary structure of the cleavage site associated with trypsin enhancement of rotavirus SA11 infectivity. *Virology* **144**, 11-19 (1985).

186. Maass, D. R. & Atkinson, P. H. Rotavirus proteins VP7, NS28, and VP4 form oligomeric structures. *J Virol* **64**, 2632-2641 (1990).

187. Poruchynsky, M. S., Maass, D. R. & Atkinson, P. H. Calcium depletion blocks the maturation of rotavirus by altering the oligomerization of virus-encoded proteins in the ER. *J Cell Biol* **114**, 651-656 (1991).

188. Jourdan, N. *et al.* Rotavirus is released from the apical surface of cultured human intestinal cells through nonconventional vesicular transport that bypasses the Golgi apparatus. *J Virol* **71**, 8268-8278 (1997).

189. Sapin, C. *et al.* Rafts promote assembly and atypical targeting of a nonenveloped virus, rotavirus, in Caco-2 cells. *J Virol* **76**, 4591-4602 (2002).

190. Nejmeddine, M. *et al.* Rotavirus spike protein VP4 is present at the plasma membrane and is associated with microtubules in infected cells. *J Virol* **74**, 3313-3320 (2000).

191. Antoni, F. A. Oxytocin receptors in rat adenohypophysis: evidence from radioligand binding studies. *Endocrinology* **119**, 2393-2395 (1986).

192. Hook, V. Y., Heisler, S., Sabol, S. L. & Axelrod, J. Corticotropin releasing factor stimulates adrenocorticotropin and beta-endorphin release from AtT-20 mouse pituitary tumor cells. *Biochem Biophys Res Commun* **106**, 1364-1371 (1982).

193. Lutz-Bucher, B., Jeandel, L., Heisler, S., Roberts, J. L. & Koch, B. Evidence that AVP receptors in AtT-20 corticotrophs are not coupled to secretion of POMC-derived peptides. *Mol Cell Endocrinol* **53**, 161-167 (1987).

194. Adler, M., Sabol, S. L., Busis, N. & Pant, H. C. Intracellular calcium and hormone secretion in clonal AtT-20/D16-16 anterior pituitary cells. *Cell Calcium* **10**, 467-476 (1989).

195. Leong, D. A. A complex mechanism of facilitation in pituitary ACTH cells: recent single-cell studies. *J Exp Biol* **139**, 151-168 (1988).

196. Link, H., Dayanithi, G., Fohr, K. J. & Gratzl, M. Oxytocin at physiological concentrations evokes adrenocorticotropin (ACTH) release from corticotrophs by increasing intracellular free calcium mobilized mainly from intracellular stores. Oxytocin displays synergistic or additive effects on ACTH-releasing factor or

arginine vasopressin-induced ACTH secretion, respectively. *Endocrinology* **130**, 2183-2191 (1992).

197. Vandesompele, J. *et al.* Accurate normalization of real-time quantitative RT-PCR data by geometric averaging of multiple internal control genes. *Genome Biol* **3**, 1-11 (2002).

198. Antoni, F. A. & Dayanithi, G. Evidence for distinct glucocorticoid and guanine 3',5'-monophosphate-effected inhibition of stimulated adrenocorticotropin release in vitro. *Endocrinology* **126**, 1355-1360 (1990).

199. Behrend, E. N., Compton, S. L. & Kemppainen, R. J. Characterization of Dexras1/AGS1 interactors including PRA1. Mol Biol Cell 14, 232a. 2003. Abstract

200. Thiagarajan, R. *et al.* Rab3A negatively regulates activity-dependent modulation of exocytosis in bovine adrenal chromaffin cells. *J Physiol* **555**, 439-457 (2004).

201. Sun, L., Bittner, M. A. & Holz, R. W. Rab3a binding and secretion-enhancing domains in Rim1 are separate and unique. Studies in adrenal chromaffin cells. *J Biol Chem* **276**, 12911-12917 (2001).

202. Sun, L., Bittner, M. A. & Holz, R. W. Rim and exocytosis: Rab3a-binding and secretion-enhancing domains are separate and function independently. *Ann N Y. Acad Sci* **971**, 244-247 (2002).

203. Chung, S. H., Takai, Y. & Holz, R. W. Evidence that the Rab3a-binding protein, rabphilin3a, enhances regulated secretion. Studies in adrenal chromaffin cells. *J Biol Chem* **270**, 16714-16718 (1995).

204. Chung, S. H. *et al.* The C2 domains of Rabphilin3A specifically bind phosphatidylinositol 4,5-bisphosphate containing vesicles in a Ca2+-dependent manner. In vitro characteristics and possible significance. *J Biol Chem* **273**, 10240-10248 (1998).

205. Chung, S. H., Joberty, G., Gelino, E. A., Macara, I. G. & Holz, R. W. Comparison of the effects on secretion in chromaffin and PC12 cells of Rab3 family members and mutants. Evidence that inhibitory effects are independent of direct interaction with Rabphilin3. *J Biol Chem* **274**, 18113-18120 (1999).

206. Martinez, O. *et al.* The small GTP-binding protein rab6 functions in intra-Golgi transport. *J Cell Biol* **127**, 1575-1588 (1994).

207. Takai, Y., Sasaki, T., Shirataki, H. & Nakanishi, H. Rab3A small GTP-binding protein in Ca(2+)-dependent exocytosis. *Genes Cells* **1**, 615-632 (1996).

208. Linstedt, A. D. & Hauri, H. P. Giantin, a novel conserved Golgi membrane protein containing a cytoplasmic domain of at least 350 kDa. *Mol Biol Cell* **4**, 679-693 (1993).

209. Leenders, A. G., Lopes da Silva, F. H., Ghijsen, W. E. & Verhage, M. Rab3a is involved in transport of synaptic vesicles to the active zone in mouse brain nerve terminals. *Mol Biol Cell* **12**, 3095-3102 (2001).

210. Castillo, P. E. *et al.* Rab3A is essential for mossy fibre long-term potentiation in the hippocampus. *Nature* **388**, 590-593 (1997).

211. Tanaka, S. & Kurosumi, K. A certain step of proteolytic processing of proopiomelanocortin occurs during the transition between two distinct stages of secretory granule maturation in rat anterior pituitary corticotrophs. *Endocrinology* **131**, 779-786 (1992).

212. The MGC Project Team The Status, Quality, and Expansion of the NIH Full-Length cDNA Project: The Mammalian Gene Collection (MGC). *Genome Res* **14**, 2121-2127 (2004).

213. Cool, D. R. & Loh, Y. P. Identification of a sorting signal for the regulated secretory pathway at the N-terminus of pro-opiomelanocortin. *Biochimie* **76**, 265-270 (1994).

214. Kim, J. T. *et al.* Prenylated Rab acceptor 1 (PRA1) inhibits TCF/beta-catenin signaling by binding to beta-catenin. *Biochem Biophys Res Commun* **349**, 200-208 (2006).

215. Ambros, V. The functions of animal microRNAs. *Nature* **431**, 350-355 (2004).

216. Bartel, D. P. MicroRNAs: genomics, biogenesis, mechanism, and function. *Cell* **116**, 281-297 (2004).

217. Nottrott, S., Simard, M. J. & Richter, J. D. Human let-7a miRNA blocks protein production on actively translating polyribosomes. *Nat Struct Mol Biol* **13**, 1108-1114 (2006).

218. Maroney, P. A., Yu, Y., Fisher, J. & Nilsen, T. W. Evidence that microRNAs are associated with translating messenger RNAs in human cells. *Nat Struct Mol Biol* **13**, 1102-1107 (2006).

219. Miller, E. A. *et al.* Multiple cargo binding sites on the COPII subunit Sec24p ensure capture of diverse membrane proteins into transport vesicles. *Cell* **114**, 497-509 (2003).

220. Sandmann, T., Herrmann, J. M., Dengjel, J., Schwarz, H. & Spang, A. Suppression of coatomer mutants by a new protein family with COPI and COPII

binding motifs in Saccharomyces cerevisiae. *Mol Biol Cell* **14**, 3097-3113 (2003).

221. Heidtman, M., Chen, C. Z., Collins, R. N. & Barlowe, C. A role for Yip1p in COPII vesicle biogenesis. *J Cell Biol* **163**, 57-69 (2003).

222. Barlowe, C. *et al.* COPII: a membrane coat formed by Sec proteins that drive vesicle budding from the endoplasmic reticulum. *Cell* **77**, 895-907 (1994).

223. Barlowe, C. COPII: a membrane coat that forms endoplasmic reticulum-derived vesicles. *FEBS Lett* **369**, 93-96 (1995).

224. Barlowe, C. COPII and selective export from the endoplasmic reticulum. *Biochim Biophys Acta* **1404**, 67-76 (1998).

225. Bednarek, S. Y. & Raikhel, N. V. Intracellular trafficking of secretory proteins. *Plant Mol Biol* **20**, 133-150 (1992).

226. Bednarek, S. Y., Orci, L. & Schekman, R. Traffic COPs and the formation of vesicle coats. *Trends Cell Biol* **6**, 468-473 (1996).

227. Schachter, B. S., Johnson, L. K., Baxter, J. D. & Roberts, J. L. Differential regulation by glucocorticoids of proopiomelanocortin mRNA levels in the anterior and intermediate lobes of the rat pituitary. *Endocrinology* **110**, 1442-1444 (1982).

228. Eberwine, J. H. & Roberts, J. L. Glucocorticoid regulation of pro-opiomelanocortin gene transcription in the rat pituitary. *J Biol Chem* **259**, 2166-2170 (1984).